Influence of atmospheric deposition on biogeochemical cycles in an oligotrophic ocean system

France Van Wambeke¹, Vincent Taillandier², Karine Desboeufs³, Elvira Pulido-Villena¹, Julie Dinasquet^{4,5}, Anja Engel⁶, Emilio Marañón⁷, Céline Ridame⁸, Cécile Guieu²

5

¹ Aix-Marseille Université, CNRS/INSU, Université de Toulon, IRD, Mediterranean Institute of Oceanography (MIO) UM 110, 13288, Marseille, France

² CNRS, Sorbonne Université, Laboratoire d'Océanographie de Villefranche (LOV), UMR7093, 06230 Villefranche-sur-Mer, France

10 ³LISA, UMR CNRS 7583, Université Paris-Est-Créteil, Université de Paris, Institut Pierre Simon Laplace (IPSL), Créteil, France

⁴ Sorbonne Universités, Laboratoire d'Océanographie Microbienne (LOMIC), Observatoire Océanologique, 66650, Banyuls/mer, France

⁵Marine Biology Research Division, Scripps Institution of Oceanography, UCSD, La Jolla, USA

15 ⁶GEOMAR – Helmholtz-Centre for Ocean Research, Kiel, Germany

 ⁷ Department of Ecology and Animal Biology, Universidade de Vigo, 36310 Vigo, Spain
 ⁸ Sorbonne University/CNRS/IRD/MNHN, LOCEAN: Laboratoire d'Océanographie et du Climat: Expérimentation et Approches Numériques, UMR 7159, 4 Place Jussieu – 75252 Paris Cedex 05, France

Correspondence to: France Van Wambeke (france.van-wambeke@mio.osupytheas.fr) and

20 Cécile Guieu (guieu@imev-mer.fr)

Abstract.

The surface mixed layer (ML) in the Mediterranean Sea is a well stratified domain characterized by low macro-nutrients and low chlorophyll content, for almost 6 months of the year. In this study we characterize the biogeochemical cycling of nitrogen (N) in the ML by

- 25 analysing simultaneous *in situ* measurements of atmospheric deposition, nutrients in seawater, hydrological conditions, primary production, heterotrophic prokaryotic production, N₂ fixation and leucine aminopeptidase activity. Dry deposition was continuously measured across the central and western open Mediterranean Sea and two wet deposition events were sampled, one in the Ionian Sea and one in the Algerian Basin. Along the transect, N budgets
- 30 were computed to compare the sources and sinks of N in the mixed layer. *In situ* leucine aminopeptidase activity made up 14 to 66 % of the heterotrophic prokaryotic N demand, and the N₂ fixation rate represented 1 to 4.5 % of the phytoplankton N demand. Dry atmospheric

deposition of inorganic nitrogen, estimated from dry deposition of (nitrate and ammonium) in aerosols, was higher than the N_2 fixation rates in the ML (on average 4.8-fold). The dry

- 35 atmospheric input of inorganic N represented a highly variable proportion of biological N demand in the ML among the stations, 10 82% for heterotrophic prokaryotes and 1-30% for phytoplankton. As some sites were visited during several days the evolution of biogeochemical properties in the ML and within the nutrient-depleted layers could be followed. At the Algerian Basin site, the biogeochemical consequences of a wet dust
- deposition event were monitored through high frequency sampling of CTD casts. Notably, just after the rain, nitrate was higher in the ML than in the nutrient depleted layer below. Estimates of nutrient transfer from the ML into the nutrient depleted layer could explain up to a third of the nitrate loss from the ML. Phytoplankton did not benefit directly from the atmospheric inputs into the ML, probably due to high competition with heterotrophic
- prokaryotes, also limited by N and phosphorus (P) availability at the time of this study.
 Primary producers decreased their production after the rain, but recovered their initial state of activity after a 2-day lag in the vicinity of the deep chlorophyll maximum layer.

1. Introduction

65

- 50 The Mediterranean Sea (MS) is a semi-enclosed basin characterized by active ventilation and short residence times of the newly formed waters, due to its own thermohaline circulation (Mermex Group, 2011). In terms of biogeochemistry, the MS is characterized by a long summer stratification period, a west-to-east gradient of increasing oligotrophy, and a deficit in phosphorus (P) compared to nitrogen (Mermex Group, 2011). The last feature is confirmed by
- 55 a deep N/P ratio for inorganic nutrients, higher than the Redfield ratio, that increases toward the east (Krom et al., 2004).

The relationship between photoautotrophic unicellular organisms and heterotrophic prokaryotes (competition or commensalism) is affected by the balance of light and nutrients as well as possible inputs of organic matter from river runoff or atmospheric deposition.

60 Phytoplankton generally experience P, or N limitation, or both (Thingstad et al., 2005 ; Tanaka et al., 2011, Richon et al., 2018), whereas heterotrophic prokaryotes are usually P limited, or P and organic carbon co-limited (Sala et al., 2002, Van Wambeke et al., 2002, Céa et al., 2014).

The MS continuously receives anthropogenic aerosols, originating from industrial and domestic activities around the basin and from other parts of Europe, along with pulsed natural

Supprimé: from

Supprimé: by Supprimé: a

Supprimé: 1/3

Supprimé: they

inputs from the Sahara. It is thus a natural LNLC study area, well adapted to investigate the role of ocean–atmosphere exchanges of particles and gases on marine biogeochemical cycles. Recent studies describe annual records of atmospheric deposition of trace metals and inorganic macronutrients (N, P) obtained at several locations around the MS (Markaki et al.,

- 75 2010; Guieu and Ridame, in press; Desboeufs, in press). All records show pulsed and highly variable atmospheric inputs. Recent models and observations show that atmospheric deposition of organic matter (OM) is also highly variable and that their annual inputs are of the same order of magnitude as river inputs (Djaoudi et al., 2017, Kanakidou et al., 2018; Kanakidou et al., 2020; Galetti et al., 2020). Moreover, the sum of atmospheric inputs of
- nitrate, ammonium and soluble organic nitrogen has been shown to be equivalent or higher
 than those from N₂ fixation (Sandroni et al., 2007), In addition inorganic atmospheric N
 inputs alone may also be higher than N₂ fixation rates (Bonnet et al., 2011).
 Aerosol amendments in bottles, minicosms or mesocosms have been widely used to study
 trophic transfer and potential export, as they allow natural communities to be studied under
- 85 controlled conditions (i.e. Guieu et al., 2010; Herut et al., 2016; Mescioglu et al., 2019). Both diversity and functioning of various biological compartments are impacted by aerosol additions in different waters tested in the MS (Guieu and Ridame, in press, and Figure 3 therein). Differences in the biological responses have been observed, depending on the mode of deposition simulated (wet or dry), the type of aerosols used (natural or anthropogenic) and
- 90 the *in situ* biogeochemical conditions at the time of the experiment (Guieu and Ridame, in press).

A fraction of organic carbon from aerosols is soluble, and this soluble fraction is partly available to marine heterotrophic prokaryotes (Djaoudi et al., 2020). Heterotrophic prokaryotes have the metabolic capacity to respond quickly to aerosol deposition through

95 growth and changes in community composition (Rahav et al., 2016; Pulido-Villena et al., 2008; 2014), while the phytoplankton community responds more slowly or not at all (Guieu and Ridame, in press, and reference therein).

Owing to the intrinsic limitations of experiments in enclosures, which vary depending on the volume and design (i.e. the omission of higher trophic levels, absence of turbulent mixing

100 limiting exchanges by diffusion, and wall effects) such experiments cannot fully simulate *in situ* conditions (Guieu and Ridame, in press). Thus, *in situ* observations are required to understand the consequences of aerosol deposition on biogeochemical cycling in the world's ocean. Such *in situ* studies are scarce and require dedicated, high-frequency sampling to Supprimé: of Supprimé: rates Supprimé: , Supprimé: although

Supprimé: Organic Supprimé: partly

Su	ipprimé: experimental
Su	ipprimé: size
Su	ipprimé: of enclosures
Su	ipprimé: so
Su	ipprimé: , however,

115 follow the effects of deposition on the biogeochemical processes while taking into account the water column dynamics as recently emphasized in cases studies (Pulido-Villena et al., 2008 and Rahav et al., 2016).

Hence, there is a need for sampling surveys with adaptive strategies to follow aerosol deposition events *in situ* and their impacts on biogeochemical processes, especially in the

- 120 open waters of the stratified and nutrient limited MS. The objectives of the PEACETIME project were to study fundamental processes and their interactions at the ocean–atmosphere interface following atmospheric deposition (especially of Saharan dust) in the Mediterranean Sea, and how these processes impact the functioning of the pelagic ecosystem (Guieu et al., 2020).
- 125 As atmospheric deposition affects primarily the surface mixed layer (ML), the present study focuses on the upper part of the nutrient depleted layer that extends down to the nutriclines (as defined by Du et al., 2017). During the stratification period, concentrations of nitrate and phosphate inside the ML are often below the detection limits of standard methods. However, nanomolar concentrations of nitrate (and phosphate) can now be assessed accurately through
- 130 the Long Waveguide Capillary Cell (LWCC) technique (Zhang and Chi, 2002), which permits the measurement of fine gradients inside nutrient depleted layers of the MS (Djaoudi et al., 2018).

The aims of the present study were to assess the impact of atmospheric nutrient deposition on biogeochemical processes and fluxes in the open sea during the PEACTIME cruise in the MS.

- 135 For this i) we estimated nanomolar variations of nitrate concentration in the surface mixed layer (ML) under variable inputs of dry and wet aerosol deposition and ii) we compared the aerosol-derived N inputs to the ML with biological activities: primary production, heterotrophic prokaryotic production, N₂ fixation and ectoenzymatic (leucine aminopeptidase) activity. We studied the N budgets along a zonal transect that includes 13 stations crossing the
- 140 Algerian Basin, Tyrrhenian Sea and the Ionian Sea where dry atmospheric deposition was continuously measured on board together with seawater biogeochemical, biological and physical characteristics. We finally focused on a wet deposition event that occurred in the western Algerian Basin, where we investigated the evolution of biogeochemical fluxes of both N and P and microbial activities through high frequency sampling.

Supprimé: the

145

2. Materials and Methods

2.1 Sampling strategy and measured parameters

The PEACETIME cruise (doi.org/10.17600/15000900) was conducted in the Mediterranean

- 150 Sea, from May to June 2017, along a transect extending from the Western Basin to the center of the Ionian Sea (Fig. 1). For details on the cruise strategy, see Guieu et al. (2020). Short duration stations (< 8 h, 10 stations named ST1 to ST10, Fig. 1) and long duration sites (5 days, 3 sites named TYR, ION and FAST) were occupied. Chemical composition of aerosols was quantified by continuous sampling along the whole transect. In addition, two rain events
- were sampled (Desboeufs et al., 2021) one on the 29th of May at ION, and a second one, a
 dust wet deposition event, at FAST on the 5th of June.

At least 3 CTD casts were conducted at each short station. One cast focused on the epipelagic layer (0-250 m), another on the whole water column. Two casts were carried out with a standard, CTD rosette equipped with 24 Niskin bottles (12 L), and a Sea-Bird SBE9

- underwater unit with pressure, temperature (SBE3), conductivity (SBE4), chlorophyll fluorescence (Chelsea Acquatracka) and oxygen (SBE43) sensors. A third cast, from the surface to the bottom of the water column was carried out under trace metal clean conditions using an instrumental package including a titanium rosette (hereafter TMC-rosette) mounted on a Kevlar cable and equipped with Go-Flo bottles that were sampled in a dedicated clean
- 165 lab container. The long duration sites were abbreviated as TYR (situated in the center of the Tyrrhenian Basin), ION (in the center of the Ionian Basin) and FAST (in the western Algerian Basin). These 3 sites were selected based on satellite imagery, altimetry and Lagrangian diagnostics as well as forecasted rain events (Guieu et al., 2020). At these sites, repeated casts were performed over at least 4 days with alternating CTD- and TMC- rosettes (Table 1). The
- 170 succession of CTD casts at the FAST site is numbered in days relative to a rain event sampled on board the ship. The first cast of the series was sampled 2.3 days before the rain event, and the last 2 days after. The FAST site was revisited following the study at ST10 (3.8 days after the rain event).

Primary production (PP), prokaryotic heterotrophic production (BP), heterotrophic

- 175 prokaryotic abundances (hprok), ectoenzymatic activities (leucine aminopeptidase (LAP) and alkaline phosphatase (AP)), were determined on water samples collected with the standard CTD-rosette. Dissolved inorganic nutrients, dissolved organic nitrogen (DON) and phosphorus (DOP) were measured on water samples collected using the TMC-rosette. LAP and AP were determined from two layers in the epipelagic waters (5 m depth and deep
- 180 chlorophyll maximum (DCM)) at the short stations and at the ION and TYR sites In addition,

Supprimé: this issue, in prep.), Supprimé: site Supprimé: site LAP and AP were determined at 4 depths between 0 and 20 m for 4 profiles at FAST site, to determine the variability within the ML.

2.2 Analytical methods and fluxes calculations

2.2.1 Nutrients in the atmosphere

185

Total suspended aerosol particles (TSP inlet) were collected continuously throughout the
campaign for dry deposition estimations. Aerosol sampling was carried out using filtration
units on adapted membranes for off-line chemical analysis (Tovar-Sanchez et al., 2020).
Simultaneously, water soluble fraction of the aerosols was sampled continuously, using a
Particle-into-Liquid-Sampler (PILS, Orsini et al., 2003). Moreover, two wet deposition events
were sampled, one at FAST using rain collectors with on-line filtration (porosity

0.2 μm) (details in Desbeoufs et al., 2021).
 Nitrate and ammonium concentrations in the aerosols, abbreviated in the text as NO3 and NH4 respectively, were analyzed continuously on board from May 13th, using PILS sampling coupled on-line with double way ion chromatography (PILS-IC, Metrohm, model 850 Professional IC with Metrosep A Supp 7 column for anion measurements and Metrosep C4

- 200 column for cation measurements). The temporal resolution for PILS-IC analysis was 70 min for anions and 32 min for cations. Dissolved Inorganic Nitrogen (DIN) fluxes released by dry deposition were estimated by multiplying NO3 and NH4 obtained through PILS-CI measurements (nitrite concentrations were under analytical detection limits) by the dry settling velocities of N-bearing aerosols, i.e 0.21 and 1 cm s⁻¹ for NH4 and NO3, respectively
- 205 (Kouvarakis et al., 2001). Mean NO3 and NH4 concentrations were calculated from the PILS-IC data measured (1) during the occupation of each short station lasting between 0.13 and 0.66 days (with on average 5 measurements for NO3 and 11 measurements for NH4), and (2) between two successive casts at the sites with a time lag between 0.4 and 1.21 days (with on average 15 measurements for NO3 and about 30 for NH4). At ST1, NH4 and NO3
- 210 concentrations were obtained using IC analyses following water extraction from aerosol filter sampling as the PILS-IC was not operational.

Total dissolved phosphate (TDP) concentrations were estimated from soluble P concentrations extracted from particulate aerosols collected on filters after ultrapure water extraction HR-ICP-MS analysis (Neptune Plus, Thermo Scientific ™) (Fu et al., this issue, in

215 prep) since it was generally below the detection limits of the PILS-IC technique. The frequency of TDP analysis was therefore less than for NO3 and NH4 (0.28 -1.15 days

Supprimé: the Supprimé: site Supprimé: the Supprimé: site Supprimé: this issue, in prep

1	depending on the stations). At JON, TYR and FAST, filters collected aerosols at different		Supprimé: the	
	periods including each one CTD cast, when possible.		Supprimé: sites	
l	Atmospheric deposition of soluble P was estimated by multiplying the TDP concentration by			
225	a dry settling velocity of 1 cm s ⁻¹ , except at FAST, where 3 cm s ⁻¹ was used as this value is		Supprimé: the	
	better adapted for lithogenic particles (Izquierdo et al., 2012). The dissolved fraction and		Supprimé: site	
	solution from digestion (Heimburger et al., 2012) of particulate fractions in the filters were			
	analysed by ICP-AES (Inductively Coupled Plasma Atomic Emission Spectrometry, Spectro			
	ARCOS Ametek®). The speciation organic/inorganic of TDP was determined from ICP-MS			
230	and IC analysis. DOP was estimated from the difference between TDP, obtained by ICP-MS,			
	and DIP, obtained by ion chromatography.			
	In the rain samples NO3, NH4 and dissolved inorganic phosphorus (DIP) were also			
	determined using ion chromatography following recovery of the dissolved fraction, Total		Supprimé:	
I	particulate P (TPP) and dissolved organic P (DOP) were also measured in the rain samples			
235	following the protocol used for atmospheric dust (described above). The wet deposition fluxes		Supprimé: a similar	
	of dissolved nutrients and particulate fractions were estimated from the measured		Supprimé: dust	
I	concentrations in the rain sample, multiplied by total precipitation.			
	Total precipitation was taken from the total hourly precipitation accumulated during the rain			
	event over the region from the ERA5 hourly data reanalysis (Hersbach et al., 2018). In order			
240	to incorporate the regional variability of rainfall, the total precipitation was taken from the			
	total hourly precipitation over a domain whose center is the ship with a radius of 110 km		Supprimé: and whose	
I	using the ERA5 hourly data reanalysis (Hersbach et al., 2018). ERA 5 data are available on	<hr/>	Supprimé: measures	
	regular latitude-longitude grids at $0.25^{\circ} \times 0.25^{\circ}$ resolution (Desboeufs et al., 2021, Table 3).	_	Supprimé: in prep	
	Cumulative precipitation was obtained by considering the value at the center of each grid			
245	point over the domain.			
	2.2.2 Nutrients in the water column			
	Seawater samples for standard nutrient analysis were filtered online (< 0.2 μ m, Sartorius			
	Sartrobran-P-capsule with a 0.45 μ m prefilter and a 0.2 μ m final filter) directly from the Go-			
250	Flo bottles (TMC-rosette). Samples collected in acid-washed polyethylene bottles were		Supprimé: L	
I	immediately analyzed on board. Micromolar concentrations of nitrate + nitrite (NOx) and DIP			
	were determined using a segmented flow analyzer (AAIII HR SealAnalytical©) following			
	Aminot and Kérouel (2007) with a limit of quantification (calculated as ten times the standard			
	deviation of ten measurements of the blank) of 0.050 μ M for NOx and 0.020 μ M for DIP.			

Samples for the determination of nanomolar concentrations of dissolved nutrients were collected in HDPE bottles previously cleaned with supra-pure HCl. For NOx (primarily NO3 as the nitrite fraction was mostly negligible), samples were acidified to pH 1 inside the clean container and analyzed back in the home laboratory using a spectrometric method in the

- 270 visible (540 nm), with a 1 m LWCC (Louis et al., 2015). The detection limit was 6 nM, the limit of quantification was 9 nM and the reproducibility was 8.5%. DIP was analyzed immediately after sampling using the LWCC method after Pulido-Villena et al. (2010), with a detection limit of 1 nM (Pulido-Villena et al., 2021). Total dissolved phosphorus (TDP) and nitrogen (TDN) were measured using the segmented flow analyzer technique after high-
- temperature (120 °C) persulfate wet oxidation mineralization (Pujo-Pay and Raimbault,
 1994). DON was obtained as the difference between TDN and NOx. DOP, was obtained as the difference between TDP, and DIP, Labile DOP (L-DOP) was estimated as 31% of the DOP values (Pulido-Villena et al., 2021).

Total hydrolysable amino acids (TAAs) were determined as described in detail by Van280Wambeke et al. (2021). Briefly, 1 ml of sample was hydrolyzed at 100°C for 20 h with 1 ml

of 30% HCl and then neutralized by acid evaporation. Samples were analyzed by high performance liquid chromatography in duplicate according to Dittmar et al. (2009) protocols.

2.2.3 Biological stocks and fluxes in the epipelagic waters

- Flow cytometry was used for the enumeration of autotrophic prokaryotic and eukaryotic cells, heterotrophic prokaryotes (hprok) and heterotrophic nanoflagellates (HNF). Water samples (4.5 mL) were fixed with glutaraldehyde grade I 25% (1% final concentration), flash frozen and stored at -80 °C until analysis. Counts were performed on a FACSCanto II flow cytometer (Becton Dickinson). The separation of different autotrophic populations was based on their scattering and fluorescence signals according to Marie et al. (2000). For the enumeration of hprok (Gasol and Del Giorgio, 2000), cells were stained with SYBR Green I (Invitrogen Molecular Probes). HNF staining was performed with SYBR Green I as described in Christaki et al. (2011). All cell abundances were determined from the flow rate, which was calibrated with TruCount beads (BD biosciences).
- 295 Primary production (PP) was determined at 6 layers from the shallow CTD casts (0-250 m) sampled before sun rise. Samples were inoculated with ¹⁴C-bicarbonate and incubated in ondeck incubators kept at in situ temperature by flowing surface seawater and equipped with

Supprimé: (DON)

Supprimé: (TDN) Supprimé: (NOx)

Supprimé: in

Supprimé: articulate p

various blue screens to simulate different irradiance levels. After 24 h-incubations, samples were filtered through 0.2 polycarbonate filters and treated for liquid scintillation measurement

as described in detail in Marañón et al. (2021). A temperature correction was applied as explained in Marañón et al. (2021). N₂ fixation rates (N2fix) were determined as described in Ridame et al. (2011) using 2.3 L of unfiltered seawater collected in acid-washed polycarbonate bottles and enriched with ¹⁵N2 gas (99 atom% 15N) to obtain a final enrichment of about 10 atom% excess. 24 h-incubations for N2fix were conducted under the same temperature and irradiance as the corresponding PP incubations.

To calculate heterotrophic prokaryotic production (BP) samples collected in the epipelagic layers (0-250 m) were incubated with tritiated leucine using the microcentrifuge technique as detailed in Van Wambeke et al. (2021). We used the empirical conversion factor of 1.5 ng C per pmol of incorporated leucine according to Kirchman (1993). Isotope dilution was

- 315 negligible under these saturating concentrations as periodically checked with concentration kinetics. As we only used 2 on board temperature controlled dark-incubators, a temperature correction was applied as explained in Van Wambeke et al. (2021). Ectoenzymatic activities were measured fluorometrically, using the fluorogenic model substrates L-leucine-7-amido-4methyl-coumarin (Leu-MCA) and 4-methylumbelliferyl-phosphate (MUF-P) to track
- aminopeptidase (LAP) and alkaline phosphatase (AP) activity, respectively, as described in Van Wambeke et al. (2021). Briefly, the release of MCA from Leu-MCA and MUF from MUF-P were followed by measuring the increase of fluorescence in the dark (exc/em 380/440 nm for MCA and 365/450 nm for MUF, wavelength width 5 nm) in a VARIOSCAN LUX
 microplate reader. Fluorogenic substrates were added at varying concentrations (0.025, 0.05, 0.05)
- 0.1, 0.25, 0.5 and 1 μM), in 2 ml wells in duplicate. The parameters Vm (maximum hydrolysis velocity) and Km (Michaelis-Menten constant that reflects enzyme affinity for the substrate) as well as their corresponding errors were estimated by non-linear regression using the Michaelis-Menten equation:

330

 $\mathbf{V} = \mathbf{V}\mathbf{m} \times \mathbf{S}/(\mathbf{K}\mathbf{m} + \mathbf{S})$

where V is the hydrolysis rate and S the fluorogenic substrate concentration added. <u>We used</u>
 <u>an approach similar to Hoppe et al. (1993) to compute the *in situ* hydrolysis rates for LAP and
 <u>AP.</u> We assumed that total amino acids (TAA) could be representative of dissolved proteins.
 LAP and AP *in situ* activities were thus determined substituting S by TAA and L-DOP *in situ*</u>

Supprimé: Supprimé: (0.025, 0.05, 0.1, 0.25, 0.5 and 1 μM)

Déplacé (insertion) [1] Mis en forme : Non Surlignage

Mis en forme : Police : Italique

concentrations in the Michaelis-Menten equations, respectively (Van Wambeke et al., 2021; Pulido-Villena et al, 2021).

340 **2.3. Vertical nutrient fluxes**

In the absence of concomitant turbulence measurements, the mixed layer depth (MLD) can be estimated from density profiles (e.g. de Boyer Montegut et al., 2004; D'Ortenzio et al., 2005). For this study, a MLD was determined at every CTD cast as the depth where the residual mass content (i.e., the vertical integral of the density anomaly relative to surface) was equal to

345 1 kg m⁻² (Prieur et al., 2020), with an error of estimation of 0.5 m relative to the vertical resolution of the profile (1 m).

In the Mediterranean Sea, the low nutrient availability combined with a shallow mixed layer (ML) lead to the formation of a nutrient depleted layer that extend below the ML. Hereafter, the nutrient depleted layer is referred to 'NDLb' (b for bottom or base) for NO3 and as PDLb

for DIP (Fig. 2). The base of both layers corresponds to the nitracline and phoshacline depths, respectively, estimated by the deepest isopycnal at which measurements of NO3 and DIP, respectively, reach the detection limit (Kamykowski and Zentara, 1985; Omand and Mahadevan, 2015). Both nitracline and phosphacline depth is estimated at every discrete profile from the intercept of the regression line reported in a nutrient-density diagram.
Exchanges of nutrients between the ML and NDLb or PDLb are driven by diffusion or advection (Du et al., 2017). The flux of nutrients is a one dimensional setting and can be expressed as:

 $F_{\rm NO3} = F_{\rm DIF} + F_{\rm ADV}$

360

365

The diffusive flux F_{DIF} is expressed as the gradient of nutrient concentration times a vertical diffusivity coefficient K_{zz}

 $F_{DIF} = K_z x (NO3_{ML} - NO3_{NDLb}) / MLD$

The typical magnitude of K_z in the surface layers of the PEACETIME stations was assessed to be $10^{-5} \text{ m}^2 \text{ s}^{-1}$, as discussed in Taillandier et al. (2020).

The advective flux F_{ADV} is driven by the entrainment of deeper water in the mixed layer due to the erosion of the near-surface pycnocline, conversely to the detrainment of waters below the mixed layer by restratification, dependent on wind stress and heat flux (Cullen et al., 2002). It is expressed as the variation in the nutrient concentration across the ML times the temporal variation of the MLD, as:

 $F_{ADV} = (NO3_{ML} - NO3_{NDLb}) \ x \ dMLD \ / \ dt$

Supprimé: . This layer vertically extends between the MLD and the nitracline (phosphacline) depth Supprimé: latter interface Supprimé: is Supprimé: the depth of NO3 (DIP) depletion, which is Supprimé: micromolar Supprimé: Supprimé: (Supprimé:) is Supprimé: zero Supprimé: The NO3 (DIP) depletion Supprimé: of micromolar NO3 (DIP) concentration by Supprimé: There are various mechanisms, dynamical or biological, that can trigger e Supprimé: Supprimé: (Supprimé:). Using the hypothesis of vertical (one-dimensional) regimes, there are two processes of exchange Supprimé: Supprimé: by Supprimé: as Supprimé: corresponds either to Supprimé: or Supprimé: depending Supprimé: the variations in Supprimé: solar Supprimé: ing

Shallow MLs as the ones observed in this study (10 - 20 m) are primarily influenced by wind bursts that can lead to intermittent variations of the MLD, of up to several meters per day (10⁻

- 405 5 m s⁻¹). The resulting advective fluxes provide transient exchanges that are one order of magnitude greater than well-established diffusive fluxes. Over the time scale of significant atmospheric deposition events, associated rapid variations of the MLD would rather promote the input of atmospheric nutrients to be exported below the ML by advection rather than by diffusion. In other terms, using the hypothesis of non-stationary regimes due to rapid changes
- 410 in atmospheric conditions (that control both the mixing state of the ML and atmospheric nutrient inputs), we assume that vertical advection is the main process of exchange. At short stations, only single casts were carried out, preventing any estimation of temporal variations of the MLD (dMLD/dt) required for the calculation of vertical advective fluxes. Thus only a qualitative assessment of nutrient fluxes across ML is given. Vertical
- 415

distributions of DIP, along the longitudinal transect, are described in detail in a companion paper (Pulido-Villena et al., 2021).

2.4 Budget from the metabolic fluxes

Trapezoidal integration was used to integrate BP, PP and N2fix within the ML. The biological 420 activity at the surface was considered to be equal to that of the first layer sampled (around 5 m depth at the short stations, 1 m depth at FAST). When the base of the ML was not sampled, the value at that depth were estimated through linear interpolation between the 2 closest data points above and below the MLD.

For LAP, the transformation of *in situ* rates expressed in nmol TAA hydrolyzed L⁻¹ h⁻¹ were 425 transformed into nitrogen units using N per mole TAA, as the molar distributions of TAA were available. Integrated in situ LAP hydrolysis rates were calculated assuming the Michaelis-Menten parameters Vm and Km obtained at a 5 m depth to be representative of the whole ML. Thus an average in situ volumetric LAP flux in the ML was obtained by combining the average TAA concentrations in the ML with these kinetic parameters, and

430 multiplying this volumetric rate by the MLD. Daily BP, AP and LAP integrated activities were calculated from hourly rates x 24. Assuming no direct excretion of nitrogen or phosphorus, the C/N and C/P ratios of cell demand are equivalent to the cellular ratios. We used molar C/N ratios derived from Moreno and Martiny (2018) (range 6-8, mean 7) for phytoplankton and from Nagata et al. (1986) for heterotrophic prokaryotes (range 6.2-8.4, 435 mean 7.3). C/P of cyanobacteria and picophytoeukaryotes in P depleted conditions ranged

Supprimé: in the MLD Supprimé: R Supprimé: . As a consequence, o Supprimé: a

Supprimé: At the short stations and sites, the term $NO3_{ML} - NO3_{NDLb}$ can be inferred by the difference between mean nanomolar (LWCC) concentrations within the NDLb and the ML.

Supprimé: at short stations

Supprimé: as advective fluxes could not be characterized,

Supprimé: When $NO3_{ML} - NO3_{NDLb} < 0$, the NDLb is supplied with NO3 across the nutricline, and could be then possibly transferred into the ML. This means that nutrients within the ML are impacted by inputs from below. When NO3_{ML}- NO3_{NDLb} > 0, the ML is supplied in NO3 from the atmosphere which is further exported into the NDLb.

Supprimé: the

Supprimé: site

Supprimé: D

Supprimé: olumetric activity

Supprimé: was

Supprimé: ly

Supprimé: ted

Déplacé vers le haut [1]: We used an approach similar to Hoppe et al. (1993) to compute the *in situ* hydrolysis rates for LAP and AP.

Mis en forme : Surlignage

Supprimé: We assumed that total amino cids (TAA) could be representative of dissolved proteins. In situ hydrolysis rates of LAP and AP were determined using molar concentrations of TAA and L-DOP, respectively and used as the substrate concentration in the Michaelis-Menten kinetics.

Supprimé: then

Supprimé: either

Supprimé: quota

Supprimé: is

Supprimé: biomass quotas

Supprimé: sorted cells (

Supprimé:

Supprimé:)

485

from 107 to 161 (Martiny et al., 2013), Based on these we used a mean C/P of 130 for phytoplankton. A C/P value of 100 was used for heterotrophic prokaryotes (Godwin and Cotner, 2015).

Supprimé: ,

S	supprimé:	and
\sim		

J	Su	pp	rim	é: (consid	erec

3. Results

- 3.1 Nutrient patterns and biological fluxes along the PEACETIME transect
 During our study, MLD ranged between 7 m (at ST9) and 21 m (at ST1, Table S1, Fig. 3).
 The nitracline was shallow in the Provençal Basin (50 60 m), 70 m in the Eastern Algerian and Tyrrhenian Seas; further deepening in the Western Algerian and Ionian Seas (80 90 m, Table S1). Mean NO3 concentrations in the NDLb ranged from the quantification limit (9
- nM) to 116 nM (Table S1, Fig. 4). In the ML, mean NO3 concentrations ranged from 9 to 135
 nM. stations were grouped according NO3 concentrations (Table S1). Weak gradients, and therefore low exchange, between the ML and NDLb characterized stations in 'groups' 1 to 3. Stations in, 'group' 4, showed high and moderate NO3 concentrations, within the ML and NDLb, respectively, with a large positive difference (> 20 nM) between both, layers, At 5 m depth, Vm for Jeucine aminopeptidase (LAP), ranged from 0.21 to 0.56 nmol MCA-leu
- hydrolyzed $l^{-1} h^{-1}$, and Km from 0.12 to 1.29 μ M. The mean TAA within the ML ranged from 0.17 to 0.28 μ M. The mean *in situ* LAP hydrolysis rate within the ML, derived from these parameters, ranged from 0.07 to 0.29 nmol N $l^{-1} h^{-1}$ (results not shown but detailed in Van Wambeke et al., 2021).
- 505 The vertical distributions of PP and BP for the short stations are described in Marañon et al. (2021). Briefly, PP exhibited a deep maximum close to the DCM depth or slightly above whereas vertical distribution of BP generally showed 2 maxima, one within the mixed layer, and a second close to the DCM. Integrated PP (Table 1, Table S2) ranged from 138 (TYR17 May) to 284 (SD1) mg C m⁻² d⁻¹. Integrated BP (0-200 m) ranged from 44 (ION27May) to 113 (FAST+0.53) mg C m⁻² d⁻¹. Overall, at the time of the PEACETIME cruise, the transect exhibited the typical west-east gradient of increasing oligotrophy detected by ocean colour
 - (see Fig. 8 in Guieu et al., 2020),

3.2 N budgets and fluxes at short stations

515 Biological rates (all expressed in N units) within the ML at the short stations are shown in. Table 2, Phytoplankton N demand (phytoN demand) was the Jargest, followed by that of

-{	Supprimé: The
-	Supprimé: (
-	Supprimé: dropping to
-{	Supprimé: becoming
1	Supprimé: r

Supprimé: For the 'group 1' stations (see Table S1),

Supprimé: were low (below 50 nM) both within the ML and the NDLb, with weak gradient between the two layers. For the 'group 2' stations, NO3 concentrations were moderate (50 - 80 nM) both within the ML and the NDLb but still exhibiting a small difference between the two layers, indicating again no significant instantaneous exchanges. For 'group 3', higher NO3 concentrations were measured in both the ML and the NDLb (> 80 nM) but the small positive differences (< 20 nM) between the two layers still indicate weak or negligible exchanges between the two layers. For Supprimé: Supprimé: Supprimé: were measured Supprimé: the Supprimé: This indicates the presence of a gradient from the ML to the NDLb. Supprimé: the

Supprime:) kinetic parameter Vm
Supprimé: LAP ranged
Supprimé: 3 series of
Supprimé: classical

	Supprimé: were compared
	Supprimé: (
1	Supprimé:)
-	Supprimé: greatest rate

	heterotrophic prokaryotes (hprokN demand). On average, phytoN demand was 2.9 (range 1.5	Supprin
	-8.1) times greater than hprokN demand. LAP hydrolysis rates represented 14 to 66 % of the	Comme 'represent
	hprokN demand (mean \pm sd : 37% \pm 19%), N ₂ fixation rates represented 1 to 4.5% of the	Supprin
560	phytoN demand (2.6% \pm 1.3%) and 3 to 11% of the hprok N demand (6.4% \pm 2.4%). $N_{\scriptscriptstyle 2}$	Supprin
	fixation rates integrated over the ML correlated slightly better with hprokN demand ($r = 0.75$)	Supprin Supprin
	than with phytoN demand ($r = 0.66$).	Contraction
	Dissolved inorganic N (DIN=NO3+NH4) solubilized from dry atmospheric deposition ranged	
	from 17 to 40 μ mol N m ⁻² d ⁻¹ with an average contribution of NO3 by 79% (Table 2). This	Supprin
565	new DIN input was similar or higher than N_2 fixation rates within the ML (from 1.3 to 11	Supprin
0.00	fold, mean 4.8-fold). On average, DIN from dry deposition represented 27% of the hprokN	Supprin
		Supprin
	demand (range 10-82%) and 11% of the phytoN demand (range 1-30%) within the ML.	
570	3.3 Biogeochemical evolution at ION	Supprin
	The ION site was occupied from May 25 to 29. Rain events in the vicinity of the ship were	Supprin
	observed on May 26 and May 29 (Desboeufs et al., 2021). On May 29 the rain event was	Supprin
	associated with a rain front extending over more than 5 000 km ² . A rain sample could be	Supprin
	taken on board on May 29th between 5:08 and 6:00 (local time), i.e. just 3 hours before the	Supprin
575	last CTD cast. The chemical composition of the rain indicated an anthropogenic origin	Supprin
	(Desboeufs et al., 2021).	Supprin
	TDP solubilized from dry atmospheric deposition decreased from 268 nmol P $m^{-2} d^{-1}$ (May 25	
	- 26) to 124 nmol P m ⁻² d ⁻¹ (May 27-28). DIN fluxes from dry atmospheric deposition	Supprin
	averaged 29 \pm 4 µmol N m ⁻² d ⁻¹ with small variability during the occupation of the site (Table	
580	S2). The molar ratio of DIN/DIP in the rain was 208 and DOP represented 60% of the total	
500		Supprin
	dissolved P (Table 3).	studies,
	CTD casts were taken each 24 h for biological fluxes or every 48 h for DIP and NO3. Thus	Supprin
	the temporal evolution for nutrients in the water column at ION is given only by three	Supprin Supprin
	profiles. The first profile (May 25 before the rain events in the area) made during smooth	Supprin
585	weather conditions shows a shallow ML with low and homogeneous concentrations of NO3	Supprin
	in the ML and the NDLb (Fig. 4). Shortly after, rain events were observed in the area on May	depressio Supprin
	26 although not at the ship's position and the ML started to deepen 13 h before the second	Supprin
	cast sampled for nutrients (on May 27) and NO3 concentrations increases in the ML and	Supprin
	NDLb Fig. 3). While NO3 concentrations increased in the ML, the effect on the MLD was	Supprin
		Supprin in the MI

Supprimé: ic N demand Commentaire [vw1]: I pprefer to keep 'represented' Supprimé: that of Supprimé: between Supprimé: and Supprimé: between

Supprimé: of	
Supprimé: which	
Supprimé: on average were NO3	
Supprimé: the new	

Supprimé: the	
Supprimé: site	
Supprimé: this issue, in prep	
Supprimé: the	
Supprimé: covering	
Supprimé: background influence	

Supprimé: this issue, in prep.

Supprimé: -

Supprimé: ¶
Supprimé: , dedicated to biogeochemical studies,
Supprimé: time sequence
Supprimé: for
Supprimé: is 'flat', corresponding to
Supprimé: and
Supprimé: there was an atmospheric depression: some
Supprimé: but
Supprimé: on board
Supprimé: with
Supprimé: sampling
Supprimé: . This cast reflected high NO3 in the ML (

still moderate as wind conditions rose to 20 kt just at the time of the cast (Fig. 3). The interval between the second and the third cast (May 29, cast done 3 hours after the rain sampled on board) was marked by a slight decrease in wind speed, a deepening of the ML down to 18 m.

625 and a decrease in NO3 both in the ML and NDLb, with comparatively higher NO3 concentrations in ML than in the NDLb. The calculation of vertical advective fluxes between the two layers showed a downward flux in the first interval May 25-27 (Fig. 4, Table S1) and an upward flux in the second interval (May 27-29).

Due to the lack of high frequency sampling, it was not possible to quantitatively assess the effects of dry/wet atmospheric deposition nor the one of nitrate injection from below the 630 NDLd by vertical advection at ION. The intrusion of a low-salinity lens was clearly visible on the thermosalinograph record and on the 27 May CTD cast, down to 10 m depth (data not shown). This low-salinity lens could be formed by the rain event noted on 26 May in the vicinity of the station. It was clear that ION on days May 27 and 29 was characteristic of 635 group 4 (i.e. higher NO3 concentrations in the ML than in the NDLb), presumably related to NO3 rainfall inputs Vm of LAP measured on May 25 at 5 m (0.22 nmol N l⁻¹ h⁻¹) was one of the lowest values recorded during the cruise whilst Vm of AP was the highest (5.6 nmol P I^{-1} h^{-1}). PP integrated over the euphotic zone increased slightly from 188 to 226 mg C m⁻² d⁻¹ (Table S2), but due to the variability in the MLD at ION this trend was not visible when integrating PP over the ML. In the ML, BP increased slightly, from 7.5 to 10.3 mg C m⁻² d⁻¹ 640 between May 25 and May 29, indicating that hprok benefited slightly more from the atmospheric inputs than the autotrophs (Fig. S1, Table S2). The profiles of hprok and Synechococcus abundances showed no particular trend with time, with larger variations within the DCM (Fig. S1).

645

650

3.4 N budgets and fluxes at FAST,

During the occupation of FAST, two rains episodes took place starting on the evening of June 2 to the June 3 at night and in the early morning of June 5 (Tovar-Sanchez et al., 2020). The radar data indicated the presence of a rain front with patchy, numerous and intense rain events occurring over a large area surrounding the ship's location. These two episodes coincided with a dust plume transported in altitude (between 1 and 4 km) and resulted in wet deposition of dust (Desboeufs et al., 2021). A rain sample was collected on board on June 5th (between 02:36 and 03:04, local time) and was associated with a dust wet deposition flux of ~ 40 mg m⁻². The DIN/DIP ratio in the rain reached 480 (Table 3). After the rain, daily fluxes of DIN

Supprimé: The mixing should have set up a homogeneous ML, but Supprimé: sampling nutrients Supprimé: relaxation of weather depression Supprimé: and Supprimé: 20 Supprimé: Supprimé: This cast reflected Supprimé: decrease in Supprimé: but Supprimé: higher Supprimé: also particularly difficult Supprimé: direct time evolution Supprimé: the Supprimé: the Supprimé: site. Supprimé: Nevertheless, i **Supprimé:** from the casts sampled on the Supprimé: , that this site Supprimé: suggesting recent inputs from Supprimé: Supprimé: the atmosphere. Supprimé: Ectoenzymatic activities were only sampled on May 25. Supprimé: changes Supprimé: the Supprimé: site (range 11-21 m) Supprimé: tegrated over Supprimé: and Supprimé: ed Supprimé: as PP decreased at 5m depth Supprimé: high

1	Supprimé: the
-{	Supprimé: site
-(Supprimé: the
1	Supprimé: site
Y	Supprimé: :
Y	Supprimé: -night of
1	Supprimé: rain

Supprimé: this issue, in prep.).

solubilized from dry aerosol deposition strongly decreased from 61.2 to 12.9 µmol N m⁻² d⁻¹ between June 4 and 5.

The water column at FAST site before the rain event sampled on board (-2.3; -1.5; -0.25 days) 700 was marked by moderate and similar decreases in NO3 concentrations within the ML and NDLb. Integrated NO3stocks in the ML (Table S2) reflected slight changes in MLD (from 14 to 10 m during this time interval). On June 5th, the rain event (Table 3) was associated with a strong wind burst and an abrupt mixing. The comparison between NO3 concentrations from two casts, sampled 6 h before and 6 h after the rain, (FAST-0.25 and FAST+0.24), showed a 705 clear N enrichment of the ML with a mean NO3 increase from 56 to 93 nM corresponding to a NO3 integrated stocks increase by 888 µmol N m⁻² (Fig. 3, Table S2). There was also a clear difference in the mean NO3 concentrations between ML and NDLb (93 ± 15 vs 51 ± 7 nM, respectively). This is the largest NO3 difference observed during the cruise between these 2 layers (Fig. 4), confirming that the ML enrichment could not be attributed to inputs from 710 below. The relaxation of the wind burst was progressive, with a continuous deepening of the ML (Table S1). The export of the atmospheric NO3 into the NDLb was highest after the rain event (FAST+0.24). At the end of the FAST occupation period (FAST+3.8) high NO3

concentrations (mean 135 nM) were measured again within the ML.

DIP concentration dynamics were different from those of NO3, with similar DIP integrated stocks within the ML being measured 6 h before and 6 h after the rain (136 μ mol m⁻²). From then on DIP stocks progressively increased reaching a maximum (281 μ mol R m⁻²) and day

then on, DIP stocks progressively increased reaching a maximum (281 μ mol P m⁻²) one day after the rain (FAST+1).

Immediately after the rain, integrated PP (euphotic zone) decreased from 274 mg C m⁻² d⁻¹ (FAST-0.9) to 164 mg C m⁻² d⁻¹ (FAST+0.07) and continued to decrease the following day. It 720 was only 3.8 days after the rain that PP returned to initial values (Table S2). Such variations

- were mostly due to changes in <u>PP</u> within the DCM depth (Fig. S2), as the <u>values</u> did not change significantly within the ML (28-33 mg C m⁻² d⁻¹, Fig. S2, Fig. 5). Integrated BP in the upper 200 m of the water column showed the opposite trend to that of PP increasing from 86 $\pm 3 \text{ mg C m}^{-2} \text{ d}^{-1}$ (n = 4) before the rain, up to 113 mg C m⁻² d⁻¹ at FAST+0.5. (Table S2),
- Although modest, this increasing trend was also visible over the ML (12-15 to 15-19 mg C m⁻² d⁻¹ after the rain event). The abundances of picophytoplankton groups varied mostly in the vicinity of the DCM depth with peaks occurring 1-2 days after the rain (grey profiles, Fig S3),

Supprimé: 45 Supprimé: 9.8

Supprimé: beginning of the Supprimé: sampling

Supprimé: of NO3 with
Supprimé: of

-{	Supprimé: as
$\left(\right)$	Supprimé: d
1	Supprimé: and NO3
1	Supprimé: d
-{	Supprimé: high
-{	Supprimé: is
-{	Supprimé: is
-{	Supprimé: maximal
-{	Supprimé: site

Supprimé: the
Supprimé: (before the rain) of integrated PP could be observed again
Supprimé: volumetric rates
Supprimé: activity
Supprimé: over
Supprimé: 0-
Supprimé: and tended to
Supprimé: e
Supprimé: after the rain (
Supprimé: and
Supprimé: (
Supprimé:)
Supprimé: after (
Supprimé:)
Supprimé: when integrating BP only
Supprimé: before;
Supprimé: were mostly
Supprimé: ying

in particular for prokaryotes (*Prochlorococcus*, *Synechococcus*). Heterotrophic prokaryotes and nanoflagellate abundances increased slightly within the DCM depth after the rain.

765 4. Discussion

The specific context of the oceanographic survey constrained the temporal and spatial coverage of our analysis, as the biogeochemical responses to a rain event were investigated over a few days (3 - 5), and tens of km (40 - 50). Their evolution was restricted to the vertical dimension, integrating lateral exchanges by horizontal diffusion or local advection that occurred over the corresponding space and time scales. In the vertical dimension, exchanges of nutrients across the ML were controlled by mixing due to rapidly changing conditions (MLD fluctuations along with nutrient inputs from the atmosphere) rather than diffusion. Four groups of stations, corresponding to different stages of ML enrichment and relaxation, due to

the nutrient inputs from single rain events, have been characterized based on the differences in
NO3 concentration between the ML and NDLb (see section 2.4). As shown in Fig. 4, this succession of stages is in agreement with the NO3 fluxes from above and below the ML.
Moreover, they provide a temporal scaling of the oceanic response to atmospheric deposition, with a quasi-instantaneous change at the time of the rain event and a 2-day relaxation period
to recover to pre-event conditions

In this context, we will i) discuss the nitrogen budget within the ML at the short stations considered as a 'snapshot', and ii) analyze in detail, using a time series of CTD casts, the biogeochemical changes within the ML and the NDLb following the atmospheric wet deposition event at FAST, discussing the possible modes of transfer of nutrients between these 2 layers.

4.1 A snapshot of biological fluxes in the ML and their link to new DIN from atmospheric dry deposition

The dependence of hprok on nutrients rather than on labile organic carbon during
stratification conditions is not uncommon in the MS (Van Wambeke et al., 2002, Céa et al, 2017; Sala et al., 2002) and has also been shown during PEACETIME cruise (P, or N,P colimitation, Fig. S4). Hprok have an advantage due to their small cell size and their kinetic systems which are adapted to extremely low concentrations of nutrients (for example for DIP see Talarmin et al., 2015). Under such conditions of limitation, hprok will react rapidly to

Supprimé: slightly

Supprimé: prescribed
Supprimé: advection
Supprimé: to
Supprimé: between stationary pools

Supprimé: the Supprimé: site

new phosphorus and nitrogen inputs, coming from atmospheric deposition. During an artificial in situ DIP enrichment experiment in the Eastern Mediterranean, P rapidly circulated through hprok and heterotrophic ciliates, and the phytoplankton was not directly linked to this Supprimé: while 805 'bypass' process (Thingstad et al., 2005). Bioassays conducted in the tropical Atlantic Ocean have also shown that hprok respond more strongly than phytoplankton to nutrients from Saharan aerosols (Marañón et al. 2010), a pattern that has been confirmed in a meta-analysis of dust addition experiments (Guieu et al., 2014; Guieu and Ridame, in press; Gazeau et al., 2021). 810 We considered hprokN demand together with phytoN demand and compared it to autochthonous (DON hydrolysis by ectoenzymatic activity) and allochthonous (atmospheric deposition) sources. To the best of our knowledge this is the first time that these fluxes are compared based on their simultaneous quantification at sea. High variability was observed Supprimé: A h 815 among the 10 short stations (Table 2). The regeneration of nitrogen through aminopeptidase activity was clearly the primary provider of N to hprok as 14 to 66% (mean \pm sd : 37% \pm 19%) of the hprokN demand could be satisfied by in situ LAP activity. Such percentages may be largely biased by the conversion factors from C to N and propagation of errors for the LAP hydrolysis rates and BP rates. However, the C/N ratio of hprok is relatively constant even Supprimé: narrow 820 under large variations of P or N limitation (6.2 to 8.4; Nagata, 1986). Other regeneration sources exist such as direct excretion of NH4 or low molecular weight DON sources with no necessity for hydrolysis prior to uptake (Jumars et al., 1989). For instance, Feliú et al. (2020) calculated that NH4 and DIP excretion by zooplankton would satisfy 25-43% of the phytoN demand and 22-37% of the phytoP demand over the whole 825 euphotic zone. Such percentages suggest that direct excretion by zooplankton along with ectoenzymatic activity provide substantial N for biological activity. N₂ fixation is also a source of new N that can directly fuel hprok as some diazotrophs are heterotrophic (Delmont et al. 2018, and references therein), or indirectly, as part of the fixed N₂ that rapidly cycles through hprok (Caffin et al., 2018). Furthermore, it has been observed 830 that there is a better coupling of N2fixation rates with BP rather than with PP in the eastern MS (Rahav et al., 2013b). This was also observed within the ML in this study. Our data showed that the hypothetical contribution of N2fixation rates to hprokN demand within the ML was low ($6.4 \pm 2.4\%$) and consistent with the low N2fixation rates observed in the MS (i.e Rahav et al., 2013a; Ibello et al., 2010; Ridame et al., 2011; Bonnet et al., 2011). This differs

	from other parts of the ocean primarily limited by N but not by P, such as the south eastern		
	Pacific where N_2 fixation rates are high (Bonnet et al., 2017) and can represent up to 81 % of		
840	the hprokN demand (Van Wambeke et al., 2018).		
	The sum of LAP activity and N_2 fixation were not sufficient to meet hprokN demand (total		
	contribution between 19 to 73% of HbactN demand). We examined the importance of new	Supprimé: F	inally, w
	DIN from dry atmospheric deposition. Atmospheric DIN fluxes from dry deposition showed a	Supprimé: so	
I	low variability along the transect (29 \pm 7 μmol N m^{2} d^{\text{-1}} at the short stations) and were among	Supprimé: pr	resent
845	the lowest previously measured in the Mediterranean basin, ranging from 38 to 240 µmol N	Supprimé: er	nvironment
	$m^{-2} d^{-1}$ (Desboeufs, in press). It has to be noted that the fluxes measured during the	Supprimé: e	t al.
Į	PEACETIME cruise are representative of the open sea atmosphere while published fluxes		
	were measured at coastal sites where local/regional contamination contributes significantly to		
	the fluxes (Desboeufs, in press). Atmospheric deposition also delivers organic matter		
850	(Djaoudi et al., 2017, Kanakidou et al., 2018), which is bioavailable for marine hprok		
	(Djaoudi et al., 2020). Dissolved organic nitrogen (DON) released from aerosols, not		
	determined here, can be estimated from previous studies. On average in the MS, DON		
	solubilized from aerosols represents 32%. (range19 to 42%) of the total dissolved N released		
	from dry deposition (Desboeufs, in press). Considering this mean, DON released from dry		
855	deposition was estimated to range from 8 to 19 $\mu mol~N~m^{-2}~d^{-1}$ at the short duration stations.		
	The total dissolved N solubilized from dry deposition (inorganic measured +organic		
	estimated) would thus represent 14 to 121% of the hprokN demand. Because of the low		
	variability in DIN (and estimated DON) fluxes derived from dry deposition, the atmospheric		
	contribution was mainly driven by biogeochemical processes in the water column and not by	Supprimé: co	onditions
860	the variability of atmospheric fluxes during the cruise (CV of Nprok Ndemand and phyto N		
	demand at the short stations were 45% and 89%, respectively, and that of DIN flux 25%).		
	However, the calculated contribution can also be biased by the deposition velocity used to		
	calculate DIN solubilized from the dry deposition. Deposition velocity was set at 1 cm s^{-1} for		
	NO3 and 0.21 cm s ⁻¹ for NH4. As NO3 was the dominant inorganic form released by dry		
865	deposition, it is clear that the choice of 1 cm s^{-1} for NO3 influenced its contribution. This		
	choice was conditioned by the predominance of NO3 in the main types of aerosols in the	Supprimé: th Mediterranean	e large mode of
	Mediterranean basin such as dust or sea salt particles (e.g., Bardouki et al., 2003). However,	wiediterranean	
I	the deposition velocity of NO3 between fine and large particles could range from 0.6 to 2 cm		
	sec ⁻¹ in these aerosols (e.g. Sandroni et al., 2007). Even considering the lower value of 0.6 cm	Supprimé: M	Iediterranean
I			

sec⁻¹ from the literature, the contribution of DIN from atmospheric dry deposition to hprokN demand within the ML would still be significant (up to 72%).

880

4.2 Biogeochemical response after a wet deposition event – N and P budgets at FAST,	Supprimé: site
Rain events are more sporadic than dry atmospheric deposition but represent much higher	Supprimé: erratic
new nutrient fluxes to the MS surface waters on an annual basis, e.g. on average 84% of	Supprimé: on average
annual atmospheric DIN fluxes in Corsica Island (Desboeufs et al., 2018). At the scale of the	,
Mediterranean basin, the annual wet deposition of DIN was found to be 2-8 times higher that	n
DIN from dry deposition (Markaki et al., 2010). Wet deposition also contributes significantly	y
to DON atmospheric fluxes in the MS: For example at Frioul Island (Bay of Marseille, NW	
MS), total (wet + dry) DON atmospheric fluxes ranged between 7 and 367 $\mu mol \ DON \ m^{-2}$	
day ⁻¹ and represented $41 \pm 14\%$ of the total atmospheric nitrogen flux (Djaoudi et al., 2018).	
In the Eastern MS (Lampedusa Island) DON atmospheric fluxes ranged between 1.5 and 250)
µmol DON m ⁻² day ⁻¹ contributing 25% of the total atmospheric nitrogen flux, respectively	Supprimé: to
(Galletti et al., 2020). In both studies, bulk atmospheric fluxes of DON were positively	
correlated with precipitation rates, indicating the preponderance of wet over dry deposition.	Supprimé: deposition
At FAST, the maximum net variations of NO3 and DIP concentrations within the ML	Supprimé: the
before/after the rainy period reached 1520-665 = $+855 \mu mol N m^{-2}$ for NO3 and 281-137 =	Supprimé: site
+144 μ mol P m ⁻² for DIP (Table S2). In other terms, based on a mean MLD of 16 m, the net	
observed increases in the ML were + 9 nM DIP and + 54 nM NO3. These net variations	
observed in the ML are higher than the calculated variation in stocks deduced from the N and	1
P concentrations of this rain event (0.07 nM DIP and 21 nM NO3 concentrations increase	
over the whole ML (Table 3). This is still true when including all P or N chemical species	Supprimé: forms
(particulate and soluble inorganic + organic fractions) with, for example an increase in P	Supprimé: .
concentration in the ML of ~ 0.68 nM. As described in the results section 3.4, the rains	Supprimé: F
affecting the FAST site were spatially patchy over a large area (~40-50 km radius around the	Supprimé: the Supprimé: would increase by
R/V). Thus, we consider that the biogeochemical impacts observed at FAST site were	
probably due to a suite of atmospheric events rather than only the single event observed on	
board. It is also possible that meso- and sub-mesoscale dynamics encountered at FAST site	
(Figs 5 and 12 in Guieu et al., 2020) may have affected such cumulative impact.	
Interestingly, a delay of about 19 h was observed in the maximum net accumulation within	
the ML between DIP (FAST+1.05) and NO3 (FAST+0.24). The DIN/DIP ratio in the rain	

(1438) was much higher than the Redfield ratio. As the biological turnover of DIP in the MS is rapid (from minutes to few hours, Talarmin et al., 2015), new DIP from rain might have

925

945

- behaved differently than DIN. Two different mechanisms can explain this delay: (i) processes linked to bypasses and luxury DIP uptake (storage of surplus P in hprok before a rapid development of grazers (Flaten et al, 2005; Herut et al 2005, Thingstad et al., 2005) that are later responsible for DIP regeneration) so that DIP net accumulation is delayed and/or (ii)
- 930 abiotic processes such as rapid desorption from large sinking particles followed by adsorption of DIP onto submicronic iron oxides still in suspension as observed experimentally in Louis et al. (2015).

The first proposed mechanism may be supported by the observed increase of BP, along with a stable PP which suggests an immediate benefit of the new nutrients from rain to hprok rather

- than phytoplankton. The so-called luxury DIP uptake by organisms like hprok is efficient (small cells with high surface/volume ratio and DIP kinetic uptake adapted to low concentrations). It is of course difficult to quantify such *in situ* variations in comparison to mesocoms/minicosms dust addition experiments, in which clearly heterotrophy was promoted (Marañón et al., 2010; Guieu et al., 2014b; Gazeau et al., 2021). Few field studies have
- 940 confirmed these trends (Herut et al., 2005, Pulido-Villena et al., 2008) but, as stated in the introduction, these studies lacked high frequency sampling.

The second proposed mechanism, the abiotic desorption/adsorption, is compatible with the observed 19 h delay (Louis et al., 2015). Note that most of the estimates of such abiotic processes are from dust addition experiments with contrasting results, some showing this abiotic process of absorption/desorption while the particles are sinking (Louis et al., 2015),

- and others not (Carbo et al., 2005; Ridame et al., 2003). It is possible that DIP adsorbed onto large particles rapidly sinks out of the ML, and desorbs partly during its transit in the PDLb, where it could remain for longer periods due to the stratification at the pycnoclines.
 We made a tentative P budget between FAST+1.05 and FAST+2.11 where a net ML decrease jn DIP (-87 µmol P m⁻²) was observed. During this time, advective flux of DIP into the PDLb was not detectable as DIP concentrations within the ML were always lower than within the
- PDLb (Pulido-Villena et al., 2021.). This indicated that DIP was assimilated and/or transformed to DOP via biological processes, and/or adsorbed onto particles and exported to PDLb by sedimentation. By integrating PP and BP over this period (34.5 and 19.7 mg C m⁻², respectively) and assuming that the \$7 µmol DIP m⁻² removed were consumed by hprok and phytoplankton, the C/P ratio of their biomass would be 52. Such C/P suggests that DIP was

Supprimé: by Supprimé: the competing

Supprimé: is favoured first
Supprimé: attempts in the

Supprimé:) or showing it as negligible in batch experiments (
Supprimé: stay
Supprimé: thanks
Supprimé: the
Supprimé: barriers
Supprimé: of
Supprimé: in the ML
Supprimé: toward
Supprimé: the
Supprimé: then
Supprimé: on of
Supprimé: , by
Supprimé: all
Supprimé: disappearing
Supprimé:
Supprimé: would
Supprimé: be
Supprimé: a
Supprimé: reached in

not limiting these organisms anymore. Indeed a decrease of C/P quotas may highlight a switch from P to C limitation for heterotrophic bacteria (Godwin and Cotner, 2015) and from P to N limitation or increased growth rates for phytoplankton (Moreno and Martiny, 2018). Furthermore, as DIP is also recycled via alkaline phosphatase within the ML, we also

- consider another source of DIP via alkaline phosphatase activity, which could release 139
 µmol DIP m⁻² during this period (see Van Wambeke et al., 2021 for *in situ* estimates),
 Assuming also that DIP resulting from AP hydrolysis was fully assimilated by the plankton,
 the C/P ratio would be 19. This low ratio seems unrealistic for phytoplankton (Moreno and
 Martigny, 2018) as well as hprok, even growing in surplus C conditions (Makino et al., 2003;
- Lovdal et al., 2008; Godwin and Cotner, 2015).
 Some of the P recycled or brought into the ML from atmospheric deposition has consequently been exported below the ML. DIP is abiotically adsorbed on mineral dust particles (Louis et al., 2015), and is exported out of the ML while particle sedimentation. It is also possible that such processes enable the export of other P-containing organic molecules, such as DOP or
- 995 viruses produced following luxury DIP assimilation. Free viruses, richer in P than N relative to Hprok, could adsorb, like DOM, onto dust particles and constitute a P export source.
 Indeed, free viruses adsorb onto black carbon particles, possibly reducing viral infection (Mari et al., 2019; Malits et al., 2015). However, particle quality is a determining factor for DOM or microbial attachment, and what has been shown for black carbon particles is not
- 1000 necessarily true for dust particles. For instance, the addition of Saharan dust to marine coastal waters led to a negligible sorption of viruses to particles and increased abundance of free viruses (Pulido-Villena et al., 2014), possibly linked to an enhancement of lytic cycles in the ML after relieving limitation (Pradeep Ram and Sime-Ngando, 2010).

We are aware of all the assumptions made here, including (i) conversion factors, (ii) *in situ* estimates of alkaline phosphatase, (iii) some missing DIP sources in the budget, such as the excretion of zooplankton estimated to amount to 22-37% of the phytoP demand at FAST site (Feliú et al., 2020), iv) lack of knowledge on the different mechanisms linking P to dust particles, and (iv) considering the station as a 1D system. Nevertheless, all these results together suggest that both luxury consumption by Hprok and export via scavenging on

1010 mineral particles probably occurred simultaneously and could explain the observed variations of DIP in the ML.

Supprimé: *in situ* activity Supprimé: could release 139 µmol DIP m² during this period Supprimé: for P biological needs Supprimé: en

Supprimé: from

Supprimé: constitute a source of
Supprimé: the
Supprimé: sink
Supprimé: sorbing
Supprimé: on dust particles
Supprimé: s
Supprimé: for instance

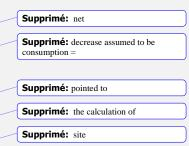
	For NO3, and in contrast to the observations for DIP, we observed physical exchanges by
	advection between the ML and NDLb. A N budget within the ML during the period of net
	NO3 decrease (between FAST+0.24, and FAST+2.11, Table S2), indicates a net loss of 1343
	μ mol N m ⁻² . For this period lasting 1.8 days, the time-integrated phytoN and hprokN demands
1030	were 682 $\mu mol~N~m^{\text{-2}}$ and 378 $\mu mol~N~m^{\text{-2}},$ respectively, so that total biological demand in the
	ML was 1060 µmol N m ⁻² . During this period, the possible N sources used were NO3 which
	decreased by $1343 \mu mol N m^{-2}$ as well as N ₂ fixation = 13 $\mu mol N m^{-2}$ and <i>in situ</i>
	aminopeptidase activity = 87 μ mol N m ⁻² . In total, these possible sources of N amounted to
	1443 µmol N m ⁻² . Keeping in mind that the same potential caveats mentioned for DIP (see
1035	above) also apply for N budget, the biological N demand appeared lower than the sources
	(difference $\sim 380 \ \mu mol \ N \ m^{-2}$). On the other hand, at FAST, vertical advective fluxes of NO3
	from ML to NDLb were up to 337 μ mol N m ⁻² d ⁻¹ (Fig. 4), i.e ~600 μ mol N m ⁻² was lost from
	the ML over 1.8 days. From these two different approaches, exported NO3 should range
	between 380 and 600 $\mu mol~N~m^{-2}$ over this period. Thus, about 40% of the NO3 accumulated
1040	in the ML after the rain was likely exported by vertical advection to the NDLb. Organisms
	present in the DCM could benefit of this input of new nutrients. Indeed, PP and abundances of
	all 4 phytoplankton groups (Synechococcus, Prochlorococcus, nano and picoeukaryotes)
	increased at the DCM after 24h and remained high for 2 days after the rain event (Fig. S3).
	The increase in abundances were higher for prokaryotic phytoplankton abundances, as such
1045	organisms would likely benefit from their small size and their ability to use DON/DOP from
	organic molecules (Yelton et al., 2016).

5. Conclusions

This study reports for the first time, in the context of an oceanographic cruise, simultaneous sampling of atmospheric and ocean biogeochemical parameters to characterize the in situ 1050 biogeochemical responses to atmospheric deposition within the ML. High-frequency sampling, in particular at FAST, confirmed the transitory state of exchanges between the ML and the NDLb. Even if dry deposition measured along the transect was homogeneous and amongst the lowest observed in the MS, that input could represent up to 121% of the hprokN demand.

1055

Our results have shown the important role played by the ML in the biogeochemical and physical processes responsible for transfers of nutrients between the atmosphere and the



Supprimé: the Supprimé: site

Supprimé: Furthermore, the signature of the dust wet deposition event on DIP and DIN concentrations was clearly detected, considering both the local rain fluxes and the horizontal oceanic mixing of water masses neighbouring waters affected by the rain front.

nutrient depleted layer below. Thanks to the use of the LWCC technique and access to nanomolar values of NO3 and DIP in repeated CTD casts, it was possible to demonstrate the 1075 role of the ML and exchanges of NO3 from the ML to the NDLb by vertical advection when variations of MLD occurred simultaneously to transitory accumulation of NO3 after a deposition event. The time sequence occurring after a wet dust deposition event was summarized as follows (Fig. 6): accumulation of NO3 in the ML, advection to NDLb, luxury consumption of DIP by hprok and delayed peaks of DIP, decrease of primary production and 1080 subsequent recovery after 2 days, mainly visible in the nutrient depleted layer. Dust deposition triggers a complex and time-controlled trophic cascade within the microbial food web. Our study shows the important role of intermittent, but strong abiotic effects such as downwelling advective fluxes from the ML to the nutrient depleted layers. It will be important to consider these aspects in biogeochemical budgets and models, especially when 1085 climate and anthropogenic changes are predicted to increase aerosol deposition in the Mediterranean Sea.

Data availability

Guieu et al., Biogeochemical dataset collected during the PEACETIME cruise. SEANOE. https://doi.org/10.17882/75747 (2020).

1090

Author contribution

CG and KD designed the study. FVW measured ectoenzymatic activity and BP, AE managed the TAA analysis and treatments, EP measured DIP with the LWCC technique, CR measured nitrogen fixation, VT assisted in CTD operations and analyzed water

1095 masses, JD sampled for DOC and flow cytometry, EM analyzed the primary production data,FVW prepared the ms with contribution from all co-authors.

Competing interests

The authors declare that they have no conflict of interest.

1100

Special issue statement

This article is part of the special issue 'Atmospheric deposition in the low-nutrient–lowchlorophyll (LNLC) ocean: effects on marine life today and in the future (ACP/BG interjournal SI)'. It is not associated with a conference. Supprimé: variations

Financial support

The project leading to this publication received funding from CNRS-INSU, IFREMER, CEA, and Météo-France as part of the program MISTRALS coordinated by INSU (doi: 10.17600/17000300) and from the European FEDER fund under project no 1166-39417. The research of EM was funded by the Spanish Ministry of Science, Innovation and

Universities through grant PGC2018-094553B-I00 (POLARIS).

Acknowledgements. This study is a contribution of the PEACETIME project

- 1115 (<u>http://peacetime-project.org</u>, last access <u>16/08/2021</u>), a joint initiative of the MERMEX and ChArMEx components. PEACETIME was endorsed as a process study by GEOTRACES and is also a contribution to IMBER and SOLAS international programs. The authors thank also many scientists & engineers for their assistance with sampling/analyses: Samuel Albani for NO3 nanomolar sampling and Maryline Montanes for
- 1120 NO3 with LWCC technique, Marc Garel, Sophie Guasco and Christian Tamburini for ectoenzymatic activity, Ruth Flerus and Birthe Zancker for TAA, Joris Guittoneau and Sandra Nunige for nutrients, Thierry Blasco for POC, Julia Uitz and Céline Dimier for TChl a (analysed at the SAPIG HPLC analytical service at the IMEV, Villefranche), María Pérez Lorenzo for primary production measurements, Philippe Catala for flow cytometry analyses,
- Barbara Marie and Ingrid Obernosterer for DOC analyses and treatments, Sylvain Triquet and Franck Fu for atmospheric particulate nitrogen and phosphorus and PEGASUS team for atmospheric sampling. Maurizio Ribera d'Alcala and a second anonymous reviewer helped much to improve this ms. We warmly thank the Co-Editor in Chief, Cristine Klass for her corrections which greatly improved the lecture of this ms.

1130

1110

References

- Aminot, A., and Kérouel, R. : Dosage automatique des nutriments dans les eaux marines, in: Méthodes d'analyses en milieu marin, edited by: IFREMER, Plouzané, 188 pp, IBSN no 978-2-7592-0023-8, 2007.
- Bardouki, H., Liakakou, H., Economou, C., Sciare, J., Smolik, J., Zdimal, V., Eleftheriadis,K., Lazaridis, M., Dye, C., and Mihalopoulos, N.: Chemical composition of size

Supprimé: 13 Supprimé: 07 resolved atmospheric aerosols in the eastern Mediterranean during summer and winter, Atmos. Environ., 37, 195–208, 2003.

- Bonnet, S., Grosso, O., and Moutin, T.: Planktonic dinitrogen fixation along a longitudinal gradient across the Mediterranean Sea during the stratified period (BOUM cruise), Biogeosciences, 8, 2257–2267, 2011.
- Bonnet, S., Caffin, M., Berthelot, H., and Moutin, T.: Hot spot of N₂ fixation in the western
 tropical South Pacific pleads for a spatial decoupling between N2 fixation and
 denitrification, PNAS letter, doi: 10.1073/pnas.1619514114, 2017.
 - Caffin, M., Berthelot, H., Cornet-Barthaux, V., Barani, A., and Bonnet, S.: Transfer of diazotroph-derived nitrogen to the planktonic food web across gradients of N₂ fixation activity and diversity in the western tropical South Pacific Ocean, Biogeosciences, 15, 3795–3810, doi: 10.5194/bg-15-3795-2018, 2018.

- Carbo, P., Krom, M. D., Homoky, W. B., Benning, L. G., and Herut, B.: Impact of atmospheric deposition on N and P geochemistry in the southeastern Levantine basin, Deep Sea Res. II, 52, 3041–3053. doi: 10.1016/j.dsr2.2005.08.014, 2005.
- Céa, B., Lefèvre, D., Chirurgien, L., Raimbault, P., Garcia, N., Charrière, B., Grégori, G.,
 Ghiglione, J.-F., Barani, A., Lafont, M., and Van Wambeke, F.: An annual survey of bacterial production, respiration and ectoenzyme activity in coastal NW Mediterranean waters: temperature and resource controls, Environ. Sci. Pollut. Res., doi: 10.1007/s11356-014-3500-9, 2014.
- Christaki, U., Courties, C., Massana, R., Catala, P., Lebaron, P., Gasol, J. M., and Zubkov,
 M.: Optimized routine flow cytometric enumeration of heterotrophic flagellates using SYBR Green I, Limnol. Oceanogr. Methods, 9, doi: 10.4319/lom.2011.9.329, 2011.
 - Cullen, J. J., Franks, P. J., Karl, D. M., and Longhurst, A. L. A. N.: Physical influences on marine ecosystem dynamics. The sea, 12, 297-336, 2002.
- de Boyer Montegut, C., Madec, G., Fisher, A. S., Lazar, A., and Iudicone, D.: Mixed layer
 depth over the global ocean: An examination of profile data and a profile-based
 climatology, Journal of Geophysical Research. Oceans, 109, C12003, doi:
 10.1029/2004JC002378, 2004.

- Delmont , T. O., Quince, C., Shaiber, A., Esen, Ö. C., Lee, S. T. M., Rappé, M. R., McLellan, S. L, Lücker, S. and Murat Eren, A.: Nitrogen-fixing populations of Planctomycetes and
 Proteobacteria are abundant in surface ocean metagenomes, Nature Microbiology, doi: 10.1038/s41564-018-0176-9, 2018.
 - Desboeufs, K.: Nutrients atmospheric deposition and variability, in: Atmospheric Chemistry and its Impacts in the Mediterranean Region (ChArMex book), Springer, in press.
- Desboeufs, K., Bon Nguyen, E., Chevaillier, S., Triquet, S., and Dulac, F.: Fluxes and sources
 of nutrient and trace metal atmospheric deposition in the northwestern Mediterranean,
 Atmospheric Chemistry and Physics, 18, 14477–14492, doi: 10.5194/acp-18-14477-2018, 2018.
 - Desboeufs, K., Fu, F., Bressac, M., Tovar-Sánchez, A., Triquet, S., Doussin, J-F., Giorio, C., Chazette, P., Disnaquet, J., Feron, A., Formenti, P., Maisonneuve, P., Rodriguez-
- Roméro, A. Zapf, P, Dulac, F., and Guieu, C.: Wet deposition in the remote western and central Mediterranean Sea as a source of trace metals to surface seawater, Atmos. Phys. Chem, Discuss. [preprint], https://doi.org/10.5194/acp-2021-624, in review, 2021,
 - Dittmar, T.H., Cherrier, J., and Ludwichowski, K.-U: The analysis of amino acids in seawater. In: Practical Guidelines for the Analysis of Seawater, edited by: Wurl, O., Boca Raton, FL: CRC-Press, 67–78, 2009.

1185

- D'Ortenzio, F., Iudicone, D., de Boyer Montegut, C., Testor, P., Antoine, D., Marullo, S.,
 Santoleri, R., and Madec, G.: Seasonal variability of the mixed layer depth in the
 Mediterranean Sea as derived from in situ profiles., Geophysical Research Letters, 32,
 L12605, doi:10.1029/2005GL022463, 2005.
- Djaoudi, K., Van Wambeke, F., Barani, A., Hélias-Nunige, S., Sempéré, R., and Pulido-Villena, E.: Atmospheric fluxes of soluble organic C, N, and P to the Mediterranean Sea: potential biogeochemical implications in the surface layer, Progress in Oceanography, 163: 59-69, MERMEX special issue, doi: 10.1016/j.pocean.2017.07.008, 2017.
- 1195 Djaoudi, K., Van Wambeke, F., Coppola, L., D'ortenzio, F., Helias-Nunige, S., Raimbault, P., Taillandier, V., Testor, P., Wagener, T., and Pulido-Villena, E.: Sensitive determination of the dissolved phosphate pool for an improved resolution of its vertical variability in

 Supprimé:

 Mis en forme : Anglais (États Unis)

 Supprimé: Wagener, T

 Supprimé: : A

 Supprimé: ?

 Supprimé: ,

 Supprimé: this special issue, in preparation.

- 1205 the surface layer: New views in the P-depleted Mediterranean Sea, Frontiers in Marine Science, vol 5, article 234, doi: 10.3389/fmars.2018.00234, 2018.
 - Djaoudi, K., Van Wambeke, F., Barani, A., Bhairy, N., Chevaillier, S., Desboeufs, K.,
 Nunige, S., Labiadh, M., Henry des Tureaux, T., Lefèvre, D., Nouara, A.,
 Panagiotopoulos, C., Tedetti, M., and Pulido-Villena E.: Potential bioavailability of organic matter from atmospheric particles to marine heterotrophic bacteria,
 - Biogeosciences, 17, 6271-6285, https://doi.org/10.5194/bg-17-6271-2020, 2020

- Du, C., Liu, Z., Kao, S.-J., and Dai, M.: Diapycnal fluxes of nutrients in an oligotrophic oceanic regime: The South China Sea, Geophysical Research Letters, 44, 11, 510–11, 518, doi: 10.1002/2017GL074921, 2017.
- 1215 Feliú, G., Pagano, M., Hidalgo, P., and Carlotti, F.: Structure and function of epipelagic mesozooplankton and their response to dust deposition events during the spring PEACETIME cruise in the Mediterranean Sea, Biogeosciences, 17, 5417–5441, https://doi.org/10.5194/bg-17-5417-2020,2020.
- Flaten, G. A., Skjoldal, E. F., Krom, M. D., Law, C. S., Mantoura, F. C., Pitta, P., Psarra, S.,
 Tanaka, T., Tselepides, A., Woodward, E. M., Zohary, T., and Thingstad, T. F.: Studies of the microbial P-cycle during a Lagrangian phosphate-addition experiment in the Eastern Mediterranean, Deep-Sea Res II, 52, 2928–2943, 2005.
- Fu, F., Desboeufs, K., Triquet, S., Doussin, J-F., Giorio, C., and Guieu, C.: Solubility and sources of trace metals associated with aerosols collected during cruise PEACETIME in
 the Mediterranean Sea, Atmos. Phys. Chem., this special issue, in preparation.
 - Galletti, Y., Becagli, S., di Sarra, A., Gonnelli, M., Pulido-Villena, E., Sferlazzo, D. M., Traversi, R., Vestri, S., and Santinelli, C.: Atmospheric deposition of organic matter at a remote site in the Central Mediterranean Sea: implications for marine ecosystem, Biogeosciences, 17, 3669–3684, https://doi.org/10.5194/bg-17-3669-2020, 2020.
- 1230 Gasol, J. M., and del Giorgio, P. A.: Using flow cytometry for counting natural planktonic bacteria and understanding the structure of planktonic bacterial communities, Scientia Marina, 64, 197–224, 2000.

- Gazeau, F., Van Wambeke, F., Marañon, E., Pérez-Lorenzo, M., Alliouane, S., Stolpe, C., Blasco, T., Leblond, N., Zäncker B., Engel A., Marie, B., Dinasquet, J., and Guieu C.:
- Impact of dust addition on the metabolism of Mediterranean plankton communities and carbon export under present and future conditions of pH and temperature,
 Biogeosciences Discuss. [preprint], https://doi.org/10.5194/bg-2021-20, in review, 2021.
- Godwin, C. M., and Cotner, J. B.: Aquatic heterotrophic bacteria have highly flexible
 phosphorus content and biomass stoichiometry, the ISME Journal, 9, 2324–2327, doi:10.1038/ismej.2015.34, 2015.
 - Guieu, C., and Ridame, C.: Impact of atmospheric deposition on marine chemistry and biogeochemistry, in: Atmospheric Chemistry and its Impacts in the Mediterranean Region (ChArMex book), Springer, in press.
- Guieu, C., Dulac, F., Desboeufs, K., Wagener, T., Pulido-Villena, E., Grisoni, J.-M., Louis, J., Ridame, C., Blain, S., Brunet, C., Bon Nguyen, E., Tran, S., Labiadh, M., and Dominici, J.-M.: Large clean mesocosms and simulated dust deposition: a new methodology to investigate responses of marine oligotrophic ecosystems to atmospheric inputs, Biogeosciences, 7, 2765–2784, doi: 10.5194/BG-7-2765-2010, 2010.
- Guieu, C., Aumont, O., Paytan, A., Bopp, L., Law, C. S., Mahowald, N., Achterberg, E. P., Marañón, E., Salihoglu, B., Crise, A., Wagener, T., Herut, B., Desboeufs, K., Kanakidou, M., Olgun, N., Peters, F., Pulido-Villena, E., Tovar-Sanchez, A., and Völker, C.: The significance of episodicity in atmospheric deposition to Low Nutrient Low Chlorophyll regions, Global Biogeochem. Cycles, 28, 1179–1198, doi:10.1002/2014GB004852, 2014a.
 - Guieu, C., Ridame, C., Pulido-Villena, E., Bressac, M., Desboeufs, K., and Dulac, F.: Impact of dust deposition on carbon budget: a tentative assessment from a mesocosm approach, Biogeosciences, 11, 5621–5635, doi: 10.5194/bg-11-5621-2014, 2014b.
- Guieu, C., D'Ortenzio, F., Dulac, F., Taillandier, V., Doglioli, A., Petrenko, A., Barrillon, S.,
 Mallet, M., Nabat, P., and Desboeufs, K.: Process studies at the air-sea interface after atmospheric deposition in the Mediterranean Sea: objectives and strategy of the

PEACETIME oceanographic campaign (May–June 2017), Biogeosciences, 17, 1–23, 2020, doi: 10.5194/bg-17-1-2020.

- Heimburger, A., Losno, R., Triquet, S., Dulac F., and Mahowald, N. M.: Direct measurements
 of atmospheric iron, cobalt and aluminium-derived dust deposition at Kerguelen
 Islands, Global Biogeochem. Cy., 26, GB4016, doi:10.1029/2012GB004301, 2012.
 - Hersbach, H., Bell, B., Berrisford, P., Biavati, G., Horányi, A., Muñoz Sabater, J., Nicolas, J.,
 Peubey, C., Radu, R., Rozum, I., Schepers, D., Simmons, A., Soci, C., Dee, D.,
 Thépaut, J-N.: ERA5 hourly data on single levels from 1979 to present. Copernicus
 Climate Change Service (C3S) Climate Data Store (CDS). doi: 10.24381/cds.adbb2d47,
 2018.
- Herut, B., Zohary, T., Krom, M. D., Mantoura, R. F. C., Pitta, P., Psarra, S., Rassoulzadegan, F., Tanaka, T. and Thingstad, T. F.: Response of East Mediterranean surface water to Saharan dust: On-board microcosm experiment and field observations, Deep-Sea
 Research II 52 (2005) 3024–3040, 2005.
- Herut, B., Rahav, E., Tsagaraki, T. M., Giannakourou, A., Tsiola, A., Psarra, S., Lagaria, A., Papageorgiou, N., Mihalopoulos, N., Theodosi, C. N., Violaki, K., Stathopoulou, E., Scoullos, M., Krom, M. D., Stockdale, A., Shi, Z., Berman-Frank, I., Meador, T. B., Tanaka, T., and Paraskevi, P.: The potential impact of Saharan dust and polluted
 aerosols on microbial populations in the East Mediterranean Sea, an overview of a mesocosm experimental approach, Front. Mar. Sci, 3, 226, doi:
 - 10.3389/fmars.2016.00226, 2016. Hoppe, H.-G., Ducklow, H., and Karrasch, B.: Evidence for dependency of bacterial growth

- on enzymatic hydrolysis of particulate organic matter in the mesopelagic ocean, Mar.
 Ecol. Prog. Ser., 93, 277–283, 1993.
 - Ibello, V., Cantoni, C., Cozzi, S., and Civitarese, G.: First basin-wide experimental results on N2 fixation in the open Mediterranean Sea, Geophys. Res. Lett., 37, L03608, doi:10.1029/2009GL041635, 2010.
- Izquierdo, R., Benítez-Nelson, C. R., Masqué, P., Castillo, S., Alastuey, A., and Àvila, A.:
 Atmospheric phosphorus deposition in a near-coastal rural site in the NE Iberian
- 29

Peninsula and its role in marine productivity, Atmos. Environ., 49, 361–370, doi: 10.1016/j.atmosenv.2011.11.007, 2012.

Jumars, P. A., Penry, D. L., Baross, J. A., Perry, M. A., and Frost, B. W.: Closing the microbial loop : dissolved carbon pathway to heterotrophic bacteria from incomplete ingestion, digestion and absorption in animals, Deep-Sea Research, 483–495, 1989.

1295

1300

- Kamykowski, D., and Zentara, S. J.: Nitrate and silicic acid in the world ocean: Patterns and processes, Mar. Ecol. Prog. Ser., 26, 47–59, 1985.
- Kanakidou, M., Myriokefalitakis, S., and Tsigaridis, K.: Aerosols in atmospheric chemistry and biogeochemical cycles of nutrients, Environ. Res. Lett., 13, 063004, doi: 10.1088/1748-9326/aabcdb, 2018.
- Kanakidou, M., Myriokefalitakis, S., and Tsagkaraki, M.: Atmospheric inputs of nutrients to the Mediterranean Sea, Deep Sea Research Part II: Topical Studies in Oceanography, 171, 104606, doi: 10.1016/j.dsr2.2019.06.014, 2020.
- Kirchman, D. L.: Leucine incorporation as a measure of biomass production by heterotrophic
 bacteria, in: Handbook of methods in aquatic microbial ecology, edited by : Kemp, P.F.,
 Sherr, B.F., Sherr, E.B., and Cole, J.J., Lewis, Boca Raton, 509-512, 1993.
 - Kouvarakis, G., Mihalopoulos, N., Tselepides, T., and Stavrakakis, S.: On the importance of atmospheric nitrogen inputs on the productivity of eastern Mediterranean, Global Biogeochemical Cycles, 15, 805–818, doi:10.1029/2001GB001399, 2001.
- 1310 Krom, M. D., Herut, B., and Mantoura, R. F. C.: Nutrient budget for the eastern Mediterranean: Implication for phosphorus limitation, Limnol. Oceanogr, 49, 1582– 1592, doi: 10.4319/lo.2004.49.5.1582, 2004.
 - Louis, J., Bressac, M., Pedrotti, M.-L., and Guieu, C.: Dissolved inorganic nitrogen and phosphorus dynamics in sea water following an artificial Saharan dust deposition event, Frontiers Marine Sci., 2, article 27, doi: 10.3389/fmars.2015.00027, 2015.
 - Løvdal, T., Skjoldal, E. F., Heldal, M., Norland, S., and Thingstad, T. F.: Changes in Morphology and Elemental Composition of Vibrio splendidus Along a Gradient from Carbon-limited to Phosphate-limited Growth, Microb. Ecol., 55, 152–161, doi: 10.1007/s00248-007-9262-x, 2008.
 - 30

 Makino, W., Cotner, J. B., Sterner, R. W., and Elser, J. J.: Are bacteria more like plants or animals? Growth rate and resource dependence of bacterial C : N : P stoichiometry, Functional Ecology, 17, 121–130, 2003.

1325

- Malits, A., Cattaneo, R., Sintes, E., Gasol, J. M., Herndl, G. J., and Weinbauer, M.: Potential impacts of black carbon on the marine microbial community, Aquat Microb Ecol., 75, 27–42, doi: 10.3354/ame01742, 2015.
- Marañón, E., Fernández, A., Mouriño-Carballido, B., Martínez-García, S., Teira, E.,
 Cermeño, P., Chouciño, P., Huete-Ortega, M., Fernández, E., Calvo-Díaz, A., Morán,
 X. A. G., Bode, A., Moreno-Ostos, E., Varela, M. M., Patey, M. D., and Achterberg, E.
 P.: Degree of oligotrophy controls the response of microbial plankton to Saharan dust,
 Limnology and Oceanography, 55, 2339–2352, 2010.
 - Marañón, E., Van Wambeke, F., Uitz, J., Boss, E. S., Dimier, C., Dinasquet, J., Angel, A.,
 Haëntjens, N., Pérez-Lorenzo, M., Taillandier, V., and Zäncker, B.: Deep maxima of
 phytoplankton biomass, primary production and bacterial production in the
 Mediterranean Sea, Biogeosciences, 18, 1749-1767, doi:10.5194/bg-18-1749-2021,
 2021.
 - Mari, X., Guinot, B., Chu, V. T., Brune, J., Lefebvre, J.-P., Pradeep Ram, A. S., Raimbault,
 P., Dittmar, T., and Niggemann, J.: Biogeochemical Impacts of a Black Carbon Wet
 Deposition Event in Halong Bay, Vietnam, Front. Mar. Sci, 6, article 185, doi:
 10.3389/fmars.2019.00185, 2019.
- 1340 Marie, D., Simon, N., Guillou, L., Partensky, F., and Vaulot, D.: Flow Cytometry Analysis of Marine Picoplankton, in: In Living Color: Protocols in Flow Cytometry and Cell Sorting, edited by: Diamond, R. A., and Demaggio, S., Springer, Berlin, Heidelberg, 421–454, 2000.
- Markaki, Z., Loye-Pilot, M. D., Violaki, K., Benyahya, L., and Mihalopoulos, N.: Variability
 of atmospheric deposition of dissolved nitrogen and phosphorus in the Mediterranean and possible link to the anomalous seawater N/P ratio, Marine Chemistry, 120, 187– 194, doi: 10.1016/j.marchem.2008.10.005, 2010.

- Martiny, A. C., Pham, C. T. A., Primeau, F. W., Vrugt, J. A., Moore, J. K., Levin, S. A., and Lomas, M. W.: Strong latitudinal patterns in the elemental ratios of marine plankton and organic matter, Nature geosciences, 6, 279–283, doi: 10.1038/ngeo1757, 2013.
 - Mermex Group.: Marine ecosystems' responses to climatic and anthropogenic forcings in the Mediterranean, Progress in Oceanography, 91, 97–166, doi: 10.1016/j.pocean.2011.02.003, 2011.
- Mescioglu E., Rahav E., Frada M.J., Rosenfeld S., Raveh O., Galletti Y., Santinelli C., Herut
 B., Paytan A.: Dust-associated airborne microbes affect primary and bacterial production rates, and eukaryote diversity, in the Northern Red Sea: A mesocosm approach. Atmosphere, 10, article 358, doi: 10.3390/atmos10070358, 2019.
 - Moreno, A. R., and Martiny, A. C.: Ecological stoichiometry of ocean plankton, Ann. Rev. Mar. Sci., 10, 43–69, 2018.
- 1360 Nagata, T.: Carbon and Nitrogen content of natural planktonic bacteria, Appl., Environ. Microbiol., 52, 28–32, 1986.
 - Orsini, D., Ma, Y., Sullivan, A., Sierau, B., Baumann, K., and Weber, R.: Refinements to the Particle-Into-Liquid Sampler (PILS) for Ground and Airborne Measurements of Water Soluble Aerosol Composition, Atmospheric Environment, 37, 1243–1259, 2003.
- Omand, M. M. and Mahadevan, A.: The shape of the oceanic nitracline, Biogeosciences, 12, 3273–3287, doi: 10.5194/bg-12-3273-2015, 2015.
 - Pradeep Ram, A. S., and Sime-Ngando, T.: Resources drive trade-off between viral lifestyles in the plankton: evidence from freshwater microbial microcosms, Environ Microbiol, 12, 467–479, doi: 10.1111/j.1462-2920.2009.02088.x, 2010.
- 1370 Prieur, L., D'Ortenzio, F., Taillandier, V. and Testor, P.: Physical oceanography of the Ligurian sea. In: Migon C., Sciandra A. & Nival P. (eds.), the Mediterranean sea in the era of global change (volume 1), evidence from 30 years of multidisciplinary study of the Ligurian sea, ISTE Sci. Publ. LTD, 49–78. doi:10.1002/9781119706960.ch3, 2020.

- 1375 Pujo-Pay, M., and Raimbault, P.: Improvements of the wet-oxidation procedure for simultaneous determination of particulate organic nitrogen and phosphorus collected on filters, Mar. Ecol. Prog. Ser., 105, 203–207, 1994.
 - Pulido-Villena, E., Wagener, T., and Guieu, C.: Bacterial response to dust pulses in the western Mediterranean: Implications for carbon cycling in the oligotrophic ocean, Global Biogeochem. Cycles, 22, GB1020, doi:10.1029/2007GB003091, 2008.
 - Pulido-Villena, E., Rérolle, V., and Guieu, C.: Transient fertilizing effect of dust in Pdeficient surface LNLC ocean. Geophysical Research Letters, 37, L01603, doi:10.1029/2009GL041415, 2010.

1380

- Pulido-Villena, E., Baudoux, A.-C., Obernosterer, I., Landa, M., Caparros, J., Catala, P.,
 Georges, C., Harmand, J., and Guieu, C.: Microbial food web dynamics in response to a Saharan dust event: results from a mesocosm study in the oligotrophic Mediterranean Sea, Biogeosciences, 11, 337–371, 2014.
- Pulido-Villena, E., Desboeufs, K., Djaoudi, K., Van Wambeke, F., Barrillon, S., Doglioli, A., Petrenko, A., Taillandier, V., Fu, F., Gaillard, T., Guasco, S., Nunige, S., Triquet, S., and Guieu, C.: Phosphorus cycling in the upper waters of the Mediterranean Sea (Peacetime cruise): relative contribution of external and internal sources, Bigeosciences Discuss., [preprint], https://doi.org/10.5194/bg-2021-94, in review, 2021.
- Rahav, E. Herut, B., Levi, A., Mulholland, M. R., and Berman-Frank, I.: Springtime
 contribution of dinitrogen fixation to primary production across the Mediterranean
 Sea. Ocean Sci. 9, 489–498. doi: 10.5194/os-9-489-2013, 2013a
 - Rahav, E., Herut, B., Stambler, N., Bar-Zeev, E. Mulholland, M. R., and Berman-Frank, I.: Uncoupling between dinitrogen fixation and primary productivity in the eastern Mediterranean Sea, J. Geophys. Res. Biogeosci., 118, 195–202, doi:10.1002/jgrg.20023, 2013b.
 - Rahav, E., Paytan, A., Chien, C.-T., Ovadia, G., Katz, T., and Herut, B.: The Impact of Atmospheric Dry Deposition Associated Microbes on the Southeastern Mediterranean Sea Surface Water following an Intense Dust Storm, Front. Mar. Sci, 3, 127, doi: 10.3389/fmars.2016.00127, 2016.

- Richon, C., Dutay, J. C., Dulac, F., Wang, R., Balkanski, Y., Nabat, P., Aumont, O., Desboeufs, K., Laurent, B., Guieu, C., Raimbault, P., and Beuvier, J.: Modeling the impacts of atmospheric deposition of nitrogen and desert dust-derived phosphorus on nutrients and biological budgets of the Mediterranean Sea, Prog. Oceanogr, 163, 21– 39, doi: 10.1016/j.pocean.2017.04.009, 2018.
- Ridame, C., Moutin, T., and C. Guieu.: Does phosphate adsorption onto Saharan dust explain the unusual N/P ratio in the Mediterranean Sea? Oceanologica Acta, 26, 629–634, doi: 10.1016/S0399-1784(03)00061-6, 2003.
 - Ridame, C., Le Moal, M., Guieu, C. Ternon, E., Biegala, I., L'Helguen, S., and Pujo-Pay, M.: Nutrient control of N₂ fixation in the oligotrophic Mediterranean Sea and the impact of Saharan dust events, Biogeosciences, 8, 2773–2783, doi:10.5194/bg-8-2773-2011, 2011.

1415

- Sala, M. M., Peters, F., Gasol, J. M., Pedros-Alio, C., Marrasse, C., and Vaque, D.: Seasonal and spatial variations in the nutrient limitation of bacterioplankton growth in the northwestern Mediterranean, Aquat. Microb. Ecol., 27, 47–56, 2002.
- Sandroni, V., Raimbault, P., Migon, C., Garcia, N., and Gouze, E.: Dry atmospheric
 deposition and diazotrophy as sources of new nitrogen to northwestern Mediterranean
 oligotrophic surface waters, Deep-Sea Res. I, 54, 1859–1870,
 doi:10.1016/j.dsr.2007.08.004, 2007.
 - Taillandier, V., Prieur, L., D'Ortenzio, F., Ribera d'Alcala, M., and Pulido-Villena, E.:
 Profiling float observation of thermohaline staircases in the western Mediterranean Sea and impact on nutrient fluxes, Biogeosciences, 17, 3343–3366, 2020.
 - Talarmin A, Van Wambeke F., Lebaron P., and Moutin T.: Vertical partitioning of phosphate uptake among picoplankton groups in the low Pi Mediterranean Sea, Biogeosciences, 12: 1237–1247 doi:10.5194/bg-12-1237-2015, 2015.
- Tanaka, T., Thingstad, T. F., Christaki, U., Colombet, J., Cornet-Barthaux, V., Courties, C.,
 Grattepanche, J.-D., Lagaria, A., Nedoma, J., Oriol, L., Psarra, S., Pujo-Pay, M., and
 Van Wambeke, F.: Lack of P-limitation of phytoplankton and heterotrophic prokaryotes in surface waters of three anticyclonic eddies in the stratified Mediterranean Sea,
 Biogeosciences, 8, 525–538, doi: 10.5194/bg-8-525-2011, 2011.

Tovar-Sánchez, A., Rodríguez-Romero, A., Engel, A., Zäncker, B., Fu, F., Marañón, E.,

- Pérez-Lorenzo, M., Bressac, M., Wagener, T., Triquet, S., Siour, G., Desboeufs, K., and Guieu, C.: Characterizing the surface microlayer in the Mediterranean Sea: trace metal concentrations and microbial plankton abundance, Biogeosciences, 17, 2349–2364, https://doi.org/10.5194/bg-17-2349-2020, 2020.
- Thingstad, T., Krom, M. D., Mantoura, F., Flaten, G., Groom, S., Herut, B., Kress, N., Law,
 C. S., Pasternak, A., Pitta, P., Psarra, S., Rassoulzadegan, F., Tanaka, T., Tselepides,
 A., Wassmann, P., Woodward, M., Riser, C., Zodiatis, G., and Zohary, T.: Nature of phosphorus limitation in the ultraoligotrophic eastern Mediterranean, Science, 309, 1068–1071, doi: 10.1126/science.1112632, 2005.
- Van Wambeke, F., Christaki, U., Giannakourou, A., Moutin, T., and Souvemerzoglou, K.:
 Longitudinal and vertical trends of bacterial limitation by phosphorus and carbon in the Mediterranean Sea, Microb. Ecol., 43, 119–133, doi: 10.1007/s00248-001-0038-4, 2002.
- Van Wambeke, F., Gimenez, A., Duhamel, S., Dupouy, C., Lefevre, D., Pujo-Pay, M., and Moutin, T.: Dynamics and controls of heterotrophic prokaryotic production in the
 western tropical South Pacific Ocean: links with diazotrophic and photosynthetic activity, Biogeosciences, 15: 2669–2689, doi: 10.5194/bg-15-2669-2018, 2018.
 - Van Wambeke, F., Pulido-Villena, E., Catala, P., Dinasquet, J., Djaoudi, K., Engel, A., Garel, M., Guasco, S., Marie, B., Nunige, S., Taillandier, V., Zäncker, B., and Tamburini, C.: Spatial patterns of ectoenzymatic kinetics in relation to biogeochemical properties in the Mediterranean Sea and the concentration of the fluorogenic substrate used, Biogeosciences, 18, 2301-2323, doi:10.5194/bg-18-2301-2021, 2021.

- Yelton, A. P., Acinas, S. G., Sunagawa, S., Bork, P., Pedros-Alio, C., Chisholm, S. W.: Global genetic capacity for mixotrophy in marine picocyanobacteria, ISME J 10:2946-2957, 2016.
- Zhang, J.-Z., and Chi, J.: Automated analysis of nano-molar concentrations of phosphate in natural waters with liquid waveguide, Environ. Sci. Technol., 36, 1048–1053, doi : 10.1021/es011094v, 2002.

Table 1. Main biogeochemical features/trophic conditions during the PEACETIME cruise. For TYR, ION and FAST sites investigated over several days, means ± sd are indicated. ITChla: Integrated total chlorophyll a (Chla + dvChla). IPP: Integrated particulate primary production; IBP: integrated heterotrophic prokaryotic production. Integrations from surface to 200 m depth for all data expect IPP, integrated down to the depth of 1% Photosynthetically Active Radiation (PAR) level.

1470

	sampling date	Lat. °N	Long. °E	Temp. at	Bottom	DCM depth	ITChl a	IPP	IBP
				5 m °C	depth m	m	mg chla m ⁻²	mg C m ⁻² d ⁻¹	$mg \ C \ m^{\text{-2}} \ d^{\text{-1}}$
ST1	May 12	41°53.5	6°20	15.7	1580	49	35.0	284	51
ST2	May 13	40°30.36	6°43.78	17.0	2830	65	32.7	148	55
ST3	May 14	39°0.8.0	7°41.0	14.3	1404	83	23.2	140	77
ST4	May 15	37°59.0	7°58.6	19.0	2770	64	29.2	182	66
ST5	May 16	38°57.2	11°1.4	19.5	2366	77	30.5	148	51
TYR	May 17-20	39°20.4	12°35.56	19.6	3395	80 ± 6	29 ± 3	170 ± 35	57 ± 3
ST6	May 22	38°48.47	14°29.97	20.0	2275	80	18.7	142	62
ST7	May 24	36°39.5	18°09.3	20.6	3627	87	24.2	158	57
ION	May 25-28	35°29.1	19°47.77	20.6	3054	97 ± 5	29 ± 2	208 ± 15	51 ± 9
ST8	May 30	36°12.6	16°37.5	20.8	3314	94	31.6	206	71
ST9	June 2	38°08.1	5°50.5	21.2	2837	91	36.1	214	64
FAST	June 2-7 and 9	37°56.8	2°54.6	21.0	2775	79 ± 8	34 ± 8	211 ± 57	92 ± 11
ST10	June 8	37°27.58	1°34.0	21.6	2770	89	28.9	nd	96

Table 2. N budget at the short stations within the surface mixed layer (ML). Integrated stocks (NO3, μ mol N m⁻²) and fluxes (heterotrophic prokaryotic N demand (hprokN demand), phytoplankton N demand (phytoN demand), in situ leucine aminopeptidase hydrolysis fluxes (LAP), dry atmospheric deposition of NO3 and NH4 (all fluxes in μ mol N m⁻² d⁻¹). Values presented as mean \pm sd. SD was calculated using propagation of errors: For hprokN demand triplicate measurements at each depth and a C/N ratio of 7.3 \pm 1.6; for phytoN demand triplicate measurements of PP at each depth and a C/N ratio of 7 \pm 1.4; for LAP the analytical TAA error and the Vm and Km errors; for N2fix the coefficient of variation was 10% for volumetric fluxes > 0.1 nmole N l⁻¹ d⁻¹ and 20% for lower values. For dry deposition, sd is based on the variability of the NO3 and NH4 concentrations solubilized from aerosols during the occupation of the station (see methods section 2.2.1). MLD: mixed layer depth. na: not available because under LWCC detection limits.

		stocks	biological fluxes			Dry deposition		
stations	MLD	NO3	phytoN demand	hprokN demand	LAP	N ₂ fixation	NO3	NH4
	m	µmol N m ⁻²	µmol N m ⁻² d ⁻¹		µmol N m ⁻² d ⁻¹			
ST1	21	na	1468 ± 325	184 ± 40	121 ± 28	14.6 ± 1.5	18.6 ± 1.4	1.5 ± 0.3
ST2	21	na	481 ± 161	163 ± 35	48 ± 24	10.7 ± 1.1	23.7 ± 2.2	4.1 ± 0.9
ST3	11	na	282 ± 82	126 ± 28	40 ± 17	7.8 ± 0.8	33.8 ± 3.6	4.7 ± 0.5
ST4	15	na	246 ± 80	132 ± 28	83 ± 20	10.7 ± 1.1	23.8 ± 2.9	6.3 ± 2.6
ST5	9	261 ± 22	112 ± 29	42 ± 9	17 ± 12	4.8 ± 0.5	27.0 ± 7.5	7.9 ± 1.8
ST6	18	162 ± 14	410 ± 116	204 ± 44	48 ± 24	9.1 ± 0.9	15.0 ± 0.6	9.3 ± 0.7
ST7	18	162 ± 14	226 ± 123	148 ± 33	83 ± 18	10.5 ± 1.1	23.6 ± 1.9	8.0 ± 1.2
ST8	14	911 ± 77	274 ± 66	130 ± 33	25 ± 8	4.3 ± 0.5	13.4 ± 1.7	3.8 ± 0.6
ST9	7	819 ± 70	259 ± 70	85 ± 22	21 ± 6	3.4 ± 0.4	27.4 ± 3.8	13.5 ± 0.8
ST10	19	2074 ± 176	495 ± 31	294 ± 64	42 ± 26	13.6 ± 1.4	23.9 ± 3.4	4.1 ± 0.4

Table 3. Characteristics and nutrient fluxes estimated in the 2 rain samples collected during

 the PEACETIME cruise at ION and FAST,

Supprimé: sites

event	Rain ION	Rain FAST
Date and local time	29/05 05:08-6:00	05/06 02:36-3:04
Estimated precipitation (mm)	3.5 ± 1.2	5.7 ± 1.4
DIP Flux nmol P m ⁻²	663 ± 227	1146 ± 290
DOP Flux nmol P m ⁻²	974 ± 334	908 ± 230
POP fluxes nmol P m ⁻²	239 ± 82	8801 ± 2227
NO3 Flux µmol N m ⁻²	67 ± 22	341 ± 86
NH4 Flux µmol N m ⁻²	71 ± 24	208 ± 53
DIN Flux µmol N m ⁻²	138 ± 47	550 ± 139

Figure legends

1495

Figure 1. Nitrate (NO3), concentrations in the aerosols along the PEACETIME transect. The locations of two rain events are indicated by large black circles. Stations ST 1 to 4 were not sampled for nutrient analysis at a nanomolar level.

Figure 2. Diagram showing the mixed layer (ML) and the bottom of the nitrate (NO3) depleted layer (NDLb), delineated by the nitracline depth and the mixed layer depth (MLD) as defined in this study.

Figure 3. a) Evolution of the wind speed during the PEACETIME cruise. The stations are indicated in yellow and dates in black. Vertical dotted lines delineate the beginning and the end of the ship's deployment at TYR, ION and FAST, The two rain events collected on board are indicated by the solid vertical red arrows and surrounding observed rain events by horizontal dashed red arrows. b) Distribution of nitrate (NO3) in the upper 100 m of the water column. The MLD (in red) and nitracline (in brown) are indicated.

Figure 4. Average concentration of nitrate (NO3) in the ML and NDLb, and NO3 flux from the ML into the NDLb. The stations have been classified into 4 groups (1 in blue, 2 in green, 3 in yellow, 4 in red, see section Results and Table S1 for definitions). Error bars indicate, standard deviation around mean values for nitrate concentrations, and error propagation for the flux from ML to NDLb using a 0.5 m uncertainty in the MLD variation.

1510

Figure 5. Evolution within the ML of heterotrophic prokaryotic production (BP), primary production (PP), heterotrophic prokaryotes (hprok) and *Synechococcus* (syn) abundances at FAST. The mixed layer depth is indicated by a red line.

1515 Figure 6. Synthetic view of biogeochemical processes and exchanges between the ML andNDLb at FAST before the rain and evolution after the rain.

Supprimé: aerosol

Supprimé: Representation of Supprimé:

Supprimé: o
Supprimé: sites
Supprimé: in
Supprimé: 0-100 m vertical d
Supprimé: with depth
Supprimé: the
Supprimé: types

Supprimé: are Supprimé: d by Supprimé: average

Supprimé: particulate

Supprimé: the Supprimé: site

Supprimé: the Supprimé: site